

UNIVERSITÄTSKLINIKUM HAMBURG-EPPENDORF

Institut für Immunologie

Direktor: Prof. Dr. Bernhard Fleischer

Molecular and functional analysis of ADP-ribosylated CD25

Dissertation

zur Erlangung des Grades eines Doktors der Medizin
an der Medizinischen Fakultät der Universität Hamburg.

Vorgelegt von

Sophie Teege, geb. Huggett
aus Hamburg

unter der Betreuung von Prof. Dr. Friedrich Nolte

Hamburg 2013

**Angenommen von der
Medizinischen Fakultät der Universität Hamburg am: 26.06.2015**

**Veröffentlicht mit Genehmigung der
Medizinischen Fakultät der Universität Hamburg.**

Prüfungsausschuss, der/die Vorsitzende: Prof. Dr. Friedrich Nolte

Prüfungsausschuss, zweite/r Gutachter/in: PD Dr. Evita Mohr

Prüfungsausschuss, dritte/r Gutachter/in: Prof. Dr. Eva Tolosa

Contents

1	Summary	4
2	Goals.....	5
3	Introduction	5
3.1	Interleukin-2 and the interleukin-2 receptor.....	5
3.2	CD25 and regulatory T cells (Tregs).....	9
3.3	ADP-ribosylation	12
4	Materials and Methods	15
4.1	Materials.....	15
4.2	Methods.....	24
5	Results	34
5.1	CD25 is a main target of ADP-ribosyltransferase 2 (ART2) on Yac-1 cells	34
5.2	ADP-ribosylation blocks IL-2 binding and signaling	35
5.3	ADP-ribosylation blocks IL-2 dependent proliferation	41
5.4	CD25 is ADP-ribosylated on arginine residues 35, 36 and 117.....	42
6	Discussion	46
7	Perspectives	49
8	Abbreviations	50
9	Bibliography.....	51
10	Acknowledgements	60
11	Curriculum vitae.....	62
12	Eidesstattliche Versicherung	63

1 Summary

NAD⁺-dependent ADP-ribosylation, one of the posttranslational protein modifications, is best known as a pathogenic mechanism of bacterial toxins. It is an enzymatic reaction, during which the ADP-ribose moiety of NAD⁺ is transferred to amino acid residues on the target protein. ART2.2 is a toxin-related arginine-specific ADP-ribosyltransferase. It is a GPI-anchored ectoenzyme that is expressed by murine T cells, especially on naive T cells and on Foxp3⁺CD4⁺CD25⁺ regulatory T cells (Tregs). During inflammation, the ART2.2 substrate NAD⁺ is released from damaged cells. ART2.2 then catalyzes ADP-ribosylation of other raft-associated proteins. Here, we identify CD25, the alpha chain of the interleukin-2 receptor (IL-2R), as a target of ART2. Using site-directed mutagenesis, we identified R35, R36 and R117 as ADP-ribosylation sites. ADP-ribosylation of CD25 inhibits binding of interleukin-2 (IL-2), the phosphorylation of STAT-5, and IL-2 dependent proliferation. As regulatory T cells constitutively express CD25, we propose that ADP-ribosylation of CD25 provides a mechanism to thwart Tregs at sites of inflammation in order to permit a more potent response of activated effector T cells.

2 Goals

The primary goal of this project was to analyze NAD⁺-dependent ADP-ribosylation of CD25, the alpha chain of the interleukin-2 receptor (IL-2R), on the functional and molecular level.

Possible consequences of this posttranslational protein modification on the function(s) of CD25 were investigated on CD25-expressing lymphoma cells and primary murine regulatory T cells. To this end, CD25-dependent signaling pathways, binding of interleukin-2 (IL-2) to the IL-2R as well as IL-2 dependent proliferation were analyzed in the absence or presence of extracellular NAD⁺.

On the molecular level, potential targets for ADP-ribosylation, i.e. arginines in the extracellular domain of CD25, were analyzed by site-directed mutagenesis. The capacity of these mutants to be ADP-ribosylated by ART2.2 was studied with radioactive NAD⁺ in co-transfected HEK-T cells.

3 Introduction

The introduction is divided into three parts. As the main focus is CD25, the alpha chain of the IL-2R, the first part outlines the role of IL-2 and the IL-2R in the immune system. The second part deals with CD25 and regulatory T cells, on which the protein is expressed. Finally, ADP-ribosylation and the enzymes catalyzing this posttranslational protein modification are introduced in more detail in the third part.

3.1 Interleukin-2 and the interleukin-2 receptor

Cytokines (also known as lymphokines and monokines) are secretory proteins that act on cells of the innate and adaptive immune system that mediate and regulate immune and inflammatory reactions. Cytokines can act either on the cell that produced the cytokine (autocrine action), a nearby cell (paracrine action) or even at a distance from the site of production (endocrine action). Therapeutically, cytokines are used as agents or as targets for antagonists in various immune and inflammatory diseases, such as anti-IL-1 therapy in rheumatic diseases (Dayer et al., 2001) or the recently developed IL-6 antagonist Tocilizumab (Navarro-Millan et al., 2012). Cytokines made by leukocytes that act on other leukocytes are called interleukins. Cytokine secretion is a transient event limited by the transcription and degradation of the cytokine-encoding mRNA. Cytokine actions are often pleiotropic, mediating diverse effector functions. Various cytokines can mediate similar effects (Dinarello, 2007, Oppenheim, 2001).

Cytokines bind to specific membrane receptors on their target cells, often with high affinities. Receptor expression is partly regulated by the cytokine itself, permitting amplification of a signal or a negative feedback. Cytokine receptors typically consist of one to three polypeptide chains carrying an extracellular portion that binds the ligand and a cytoplasmic portion that initiates intracellular signaling pathways. The effector function of cytokines is usually a change in gene expression of the target cell, resulting

in the expression of proteins and sometimes in the proliferation of the target cells. The cellular responses are tightly regulated by inhibitory mechanisms (Yasukawa et al., 2000).

IL-2 is an autocrine and paracrine growth, survival and differentiation factor of T lymphocytes. By acting on regulatory T cells, a subset of CD4⁺ T cells that constitutively express high levels of the IL-2R, IL-2 is also important for the regulation of T cell responses (see below). IL-2 is mainly produced by CD4⁺ T helper lymphocytes. It also acts on activated T cells, NK cells and B cells, promoting proliferation, increased cytokine synthesis and antibody secretion.

For some *in vitro* cell lines, such as CTLL-2 (Gillis and Smith, 1977, Gillis et al., 1978) cells or Kit 225 (Hori et al., 1987) cells, IL-2 is an essential growth factor, hence its original description as “T cell growth factor”. In this study, CTLL-2 cells are used to assess the effects of ADP-ribosylation on IL-2 dependent cell proliferation. Subsequent studies found contradictory functions of IL-2 *in vivo*, having immunostimulatory (Blattman et al., 2003, Kamimura and Bevan, 2007) but also immunoregulatory functions. One example is the promotion of activation-induced cell death (AICD) of T cells, whereby downregulating the number of T cells after the clonal expansion of an immune response (Zheng et al., 1998).

The injection of IL-2 *in vivo* in complex with specific anti-IL-2 antibodies (jes 6.1: anti-mouse IL-2 and 5344: anti-human IL-2) can direct IL-2 signaling toward CD25 whereby expanding Tregs. IL-2 in complex with other anti-IL-2 antibodies (S4B6: anti-mouse IL2 and Mab602: anti-human IL-2) directs IL-2 toward CD122/CD132, which induces vigorous expansion of CD8⁺ cytotoxic T cells and NK cells (Webster et al., 2009, Letourneau et al., Boyman et al., 2006).

The IL-2R is composed of three chains. The 3D-structure of the cytokine-receptor complex was solved in 2006 (Stauber et al., 2006). Together with the ligand IL-2, the alpha chain (Leonard et al., 1982), originally described as the Tac (T activation) antigen and later known as CD25, the beta chain (Tsuda et al., 1987), also known as CD122, and the common gamma chain (Takeshita et al., 1992), known as CD132, form the quaternary complex (Figure 3.1).

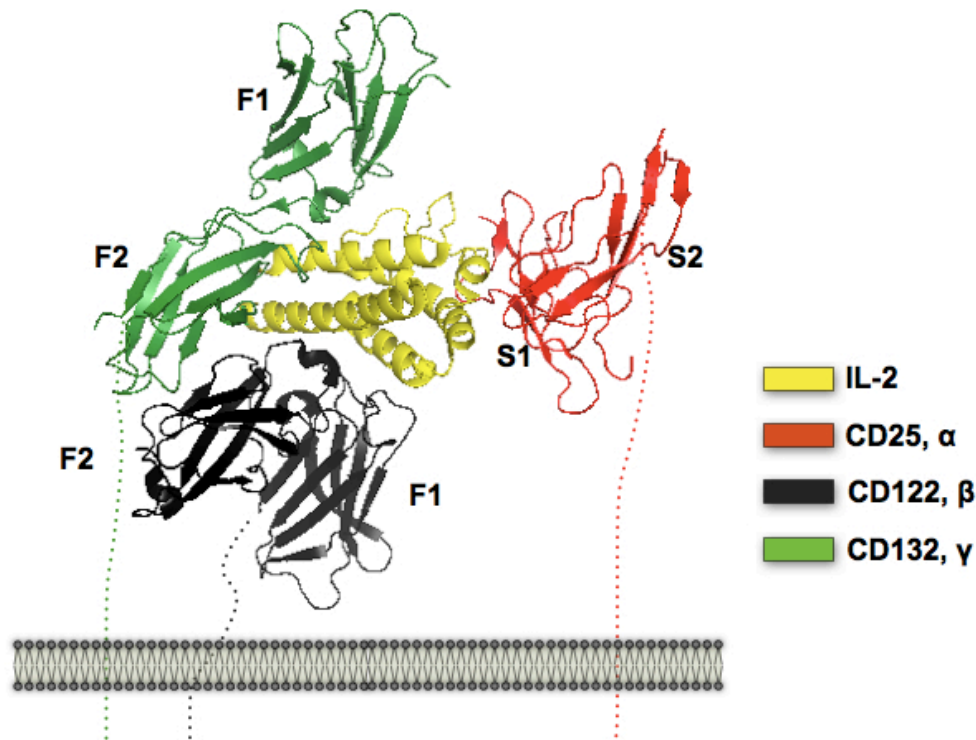


Figure 3.1: 3D cartoon model of the heterotrimeric IL-2R complex. CD25, the α chain (red), has two sushi domains (S1 and S2). CD122, the β chain (black) and CD132, also known as the common γ chain (green), have two fibronectin domains each (F1 and F2). IL-2, consisting of four α helices, is depicted in yellow. The pointed lines indicate the amino acid sequences inserting into the plasma membrane, which have not been crystallized yet. The diagram was generated with Pymol using the coordinates of the crystal structure (pdb code 2erj) (Stauber et al., 2006).

CD122 and CD132 are each composed of two fibronectin domains, while CD25 is a distinctive protein containing two “sushi” domains (Figure 3.1). All three proteins belong to the family of type I transmembrane proteins with an extracellular N-terminus and an intracellular C-terminus flanking a single transmembrane crossing. In this study, CD25 as a target protein of ADP-ribosyltransferases is studied on a molecular and functional level.

While CD25 is unique to the IL-2R complex, both CD122 and CD132 also form part of other cytokine receptors. CD132 is the γ chain of the IL-4, IL-7, IL-9, IL-15 and IL-21 receptors (Sugamura et al., 1995), while CD122 is part of the IL-15 receptor (Giri et al., 1994).

The functional IL-2R can be found in three different combinations. The α chain alone can mediate low-affinity binding ($K_d=10^{-8}$ M), but cannot transduce signals (Lin and Leonard, 1997). The β and the γ chain together form the intermediate affinity receptor ($K_d=10^{-9}$ M), which can signal in the presence of relatively high concentrations of IL-2. It is expressed on NK cells, memory CD8⁺ T cells, and resting, naïve T cells (Kovanen and Leonard, 2004). IL-15 can also act on these receptors. The high affinity receptor ($K_d=10^{-11}$ M) consists of the α , the β and the γ chain and can signal in response to relatively low concentrations of IL-2 (Theze, 1994). High affinity receptor expression is restricted to the early stages of thymocytic development, to activated mature T

lymphocytes (Rogers et al., 1997) and to regulatory T cells, which constitutively express CD25 at the highest level (Fontenot et al., 2005). By expressing the high affinity receptor, Tregs may deprive other T cells of IL-2 by binding and consuming IL-2 (Pandiyan et al., 2007).

Signal transduction of the IL-2R is mediated via the β and the γ chain (Nelson et al., 1994). IL-2 mediates the oligomerization of the γ with the β chain or the α/β chain complex (Liparoto et al., 2002, Rickert et al., 2004). Lipid raft assisted recruitment of CD25 to CD122 and CD132 has been observed (Matko et al., 2002).

IL-2 has various signal transduction pathways including the JAK-STAT, the MAP kinase and the PI3 kinase signal transduction pathways (Nelson and Willerford, 1998, Bensinger et al., 2004). In the JAK-STAT pathway, binding of IL-2 activates the JAKs (Janus family tyrosine kinases) and the phosphorylation of tyrosine residues in the intracytoplasmic domain of CD122 and CD132. The phosphorylated tyrosine residues then serve as docking sites for other signaling molecules, including STAT5 (signal transducer and activator of transcription). STAT5 is phosphorylated and dimerizes before being translocated to the nucleus to promote the transcription of target genes (Abbas et al., 2007). In this study, phosphorylation of STAT5 is used as a readout system of IL-2 signaling.

Mice and humans with immunodeficiencies resulting from mutations involved in the three chains of the IL-2R have served to further understand the *in vivo* function of those proteins. Mice deficient in the common γ chain (CD132) develop an immunodeficiency syndrome known as X-linked SCID (severe combined immunodeficiency), resulting from an extensive reduction or even absence of peripheral T and B lymphocytes (Russell et al., 1994). They have no detectable Foxp3 regulatory T cells suggesting that the common gamma chain is necessary for Foxp3 expression. In contrast, mutations in the β chain CD122 result in the constitutive activation of B and T lymphocytes causing extensive autoimmune responses that result in premature death (Suzuki et al., 1995). Mice deficient in CD25 have normal T and B cell populations at a young age whereas older mice exhibit enlarged lymphoid glands due to increased B and T cell populations and a predisposition to develop autoimmune diseases. To date, CD25 deficiency in humans has been described in two unrelated patients with recurrent infections early in life and lymphocytic infiltration in various tissues albeit normal numbers of circulating Foxp3⁺ cells (Sharfe et al., 1997, Roifman, 2000). These patients have an increased susceptibility to viral infections and a variable penetrance of endocrinopathies. They develop an intense inflammatory response to cytomegalovirus infection resulting in respiratory failure and enteropathy (Caudy et al., 2007). In 2006, a childhood case of primary biliary cirrhosis was published that also resulted from CD25 deficiency. The child suffered from a severe reduction of regulatory T cells (Aoki et al., 2006).

Pathophysiologically, CD25 deficiency hampers the negative selection of autoreactive T cells in the thymus due to a failure of T cells to down regulate the levels of the anti-apoptotic protein Bcl-2. Secondly, the inability to control autoreactive cells in the

periphery due to a dysfunctional regulatory T cell population causes the expansion of these clones explaining the extensive lymphocytic infiltration of tissues including the lung, liver, gut and bone as well as the chronic inflammatory reaction (Sharfe et al., 1997, Roifman, 2000).

Anti-CD25 antibodies have various therapeutic indications. Alongside Cyclosporin A and corticosteroids, they are used in the prevention of acute allograft rejection (Vlad et al., 2007) and in the treatment of autoimmune diseases, e.g. multiple sclerosis (Bielekova et al., 2004). Monoclonal antibodies in clinical use include daclizumab (Waldmann, 2007), a humanized mAb (90% human, 10% murine, i.e. the CDR loops) as well as basiliximab, a chimeric mAb (75% human, 25% murine, i.e. the VH and VL domains).

3.2 CD25 and regulatory T cells (Tregs)

CD25 is a type I membrane protein with a molecular weight of approximately 55kDa. Its structure reflects its exclusive ligand binding function, as it has only a short intracytoplasmic tail.

Most Tregs constitutively express CD25. Together with the transcription factor Foxp3, CD25 is used as a marker for Tregs and for Treg cell isolation (Sakaguchi et al., 1995).

Tregs are mediators of dominant self-tolerance, i.e. an active tolerance by suppressor mechanisms (in contrast to recessive tolerance in the sense of anergy). Treg cells suppress the activation, proliferation and effector functions of numerous immune effector cells *in vitro* and *in vivo*, which is essential for the prevention of autoimmune disease, immunopathology and allergy, for the maintenance of allograft tolerance and of fetal-maternal tolerance during pregnancy (Aluvihare et al., 2004). On the other hand, they may suppress immune responses against microorganisms and cancer cells (Sakaguchi et al., 2008).

The transcription factor Foxp3 is essential for development, maintenance and function of regulatory T cells (Hori et al., 2003, Fontenot et al., 2003). In addition, it acts as the Treg cell lineage specification factor (Fontenot and Rudensky, 2005). Scurfy mice, which carry a spontaneous mutation in the Foxp3 gene localized on the X chromosome, do not generate regulatory T cells and develop inflammatory disease (Brunkow et al., 2001, Wildin et al., 2001, Fontenot et al., 2003). Humans with functional Foxp3 gene mutations develop the IPEX syndrome (X linked syndrome of immunodysregulation, polyendocrinopathy and enteropathy), which is characterized by early-onset endocrinopathies such as diabetes mellitus, thyroiditis accompanied by eczema, severe allergies and enteropathy (Torgerson and Ochs, 2007, Ochs et al., 2007).

Tregs can be classified as either natural (nTregs) or induced (iTregs) (Figure 3.2). It is thought that nTregs develop in the thymus through MHC class II-dependent TCR interactions resulting in a high-avidity selection (Apostolou et al., 2002, Bensinger et al., 2001, Jordan et al., 2001). Induced Tregs develop in the peripheral organs upon specific stimulation (for example TGF-beta and retinoic acid), whereby they acquire Foxp3 expression (Curotto de Lafaille and Lafaille, 2009), which can also be simulated in *in vitro* experiments (Gavin et al., 2006).

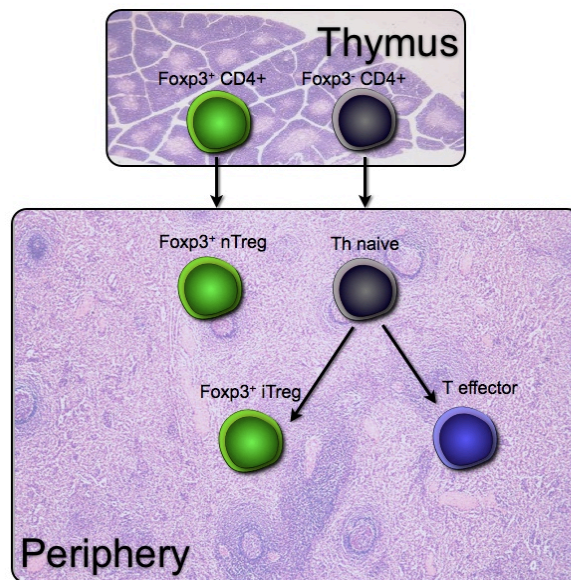


Figure 3.2: Schematic diagram of Treg development. Tregs, characterized by the expression of Foxp3, can either develop within the thymus as natural Tregs (nTregs) from Foxp3⁺CD4⁺ T cells or develop in the periphery from naïve T helper cells upon stimulation with TGF-β (transforming growth factor) and retinoic acid as induced Tregs (iTregs).

In order to specifically study the physiology of Treg cells, the transgenic DERE (‘‘depletion of regulatory T cell’’) mice were generated. These mice carry a BAC (bacterial artificial chromosome) transgene, which encodes a diphtheria toxin receptor (DTR) - enhanced green fluorescent protein (GFP) fusion protein under the control of the Foxp3 promoter (Figure 3.3). This permits the direct identification of Treg cells based on their GFP fluorescence as well as their selective depletion by the injection of diphtheria toxin (Lahl et al., 2007).

Figure 3.4 shows a FACS analysis of total splenocytes from DERE mice, after staining with fluorochrome-conjugated mAbs directed against CD4 and CD25, illustrating the good correspondence of CD25 and GFP (and thus Foxp3) expression. Panels A and B show that the proportion of the CD4⁺CD25⁺ cell population is similar to the proportion of the CD4⁺GFP⁺ population. Panel C shows that the vast majority of GFP⁺ cells expresses CD25 and panel D, gated on CD4⁺ cells, show that CD25/GFP double positive cells constitute approximately 10% of the CD4⁺ cells. In this study, DERE splenocytes are used to examine the effects of ADP-ribosylation on IL-2 signaling.

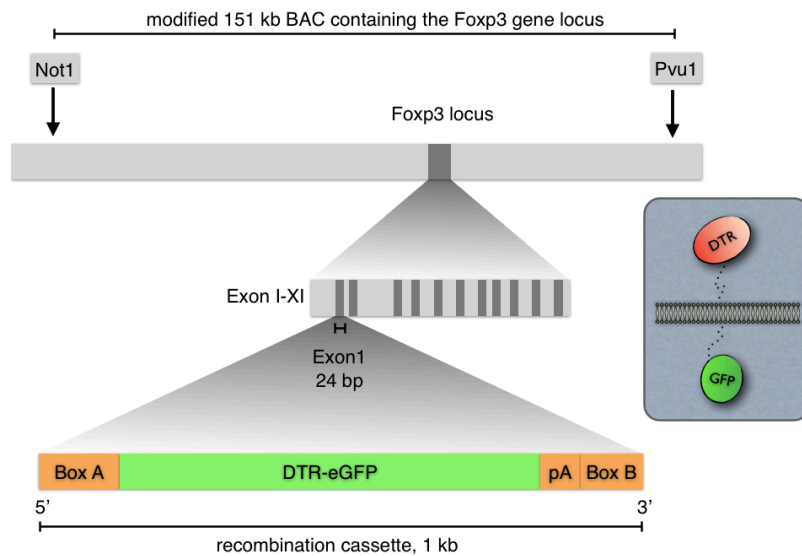


Figure 3.3: Map of the BAC construct used for generating the DEREg transgenic mice. The Foxp3 locus consists of 11 exons, of which the 24 base pairs of exon 1 were replaced by a 1-kb recombination cassette containing the gene coding for the diphtheria toxin receptor fused with eGFP (Lahl et al., 2007).

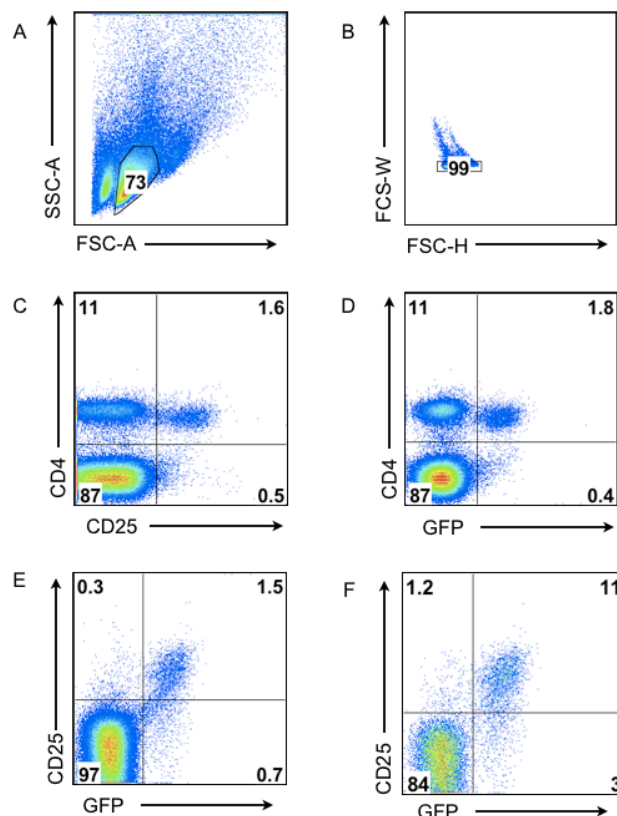


Figure 3.4: Regulatory T cell detection with flow cytometry. Primary spleen cells obtained from a DEREg mouse were stained with a V450-conjugated anti-CD4 antibody and a PE-conjugated anti-CD25 antibody. Living lymphocytes were gated in the SSC-A/FSC-A channels to exclude dead cells (panel A) as well as in the FCS-W and FSC-H view in order to exclude doublets (panel B). Panels C,D, and E show total live lymphocytes, while Figure F is gated on CD4⁺ cells.

3.3 ADP-ribosylation

ADP-ribosylation is a posttranslational modification with regulatory functions. ADP-ribosyltransferases, the enzymes that catalyze the reaction, transfer an ADP-ribose moiety from NAD^+ to specific amino acid residues on their target proteins whereby nicotinamide is released (Figure 3.5) (Seman et al., 2003, Corda and Di Girolamo, 2003, Koch-Nolte et al., 2006, Zolkiewska, 2005).

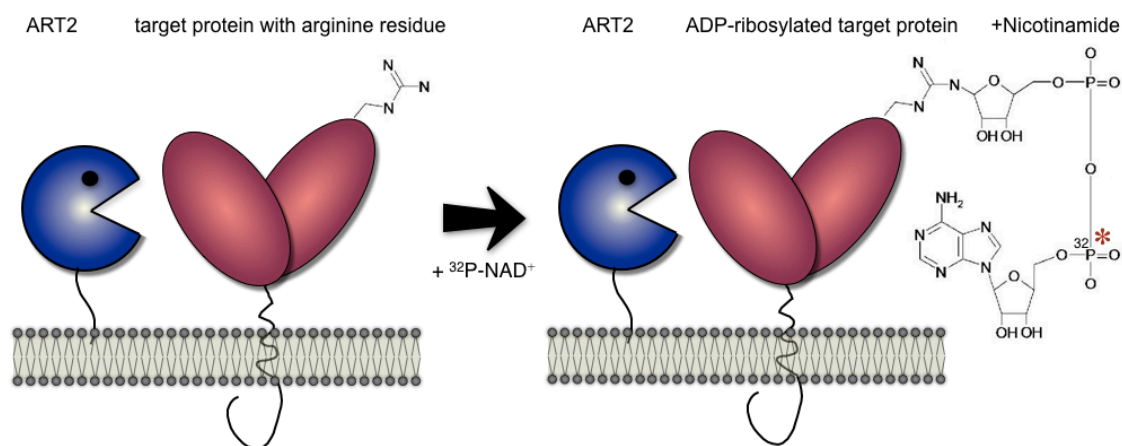


Figure 3.5: Schematic diagram of ADP-ribosylation of cell surface proteins with the radioactive substrate $^{32}\text{P-NAD}^+$. The schematic diagram shows how ADP-ribosyltransferase 2, ART2.2, modifies a target protein by ADP-ribosylation. The enzymatic reaction is arginine-specific and occurs upon availability of NAD^+ in the extracellular space, for example in inflamed tissues or $^{32}\text{P-NAD}^+$ *in vitro*. In accord with their 3D structures, the catalytic domain of ART2.2 is represented as a pacman, the two sushi domains of CD25 as a heart shaped dimer. Black lines represent the anchorage in the cell membrane – a C-terminal GPI-anchor in case of ART2.2 and a C-terminal transmembrane domain in case of CD25.

Depending on the specificity of the ADP-ribosyltransferases, the amino acids arginine, cysteine, asparagine, glutamine or diphthamide act as receptor molecules (Koch-Nolte et al., 2008, Hottiger et al., 2010). Most mammalian ecto-ADP-ribosyltransferases are arginine-specific (Koch-Nolte and Haag, 1997, Laing et al., 2010).

The extent of ADP-ribosylation is dependent on intracellular and cell-surface NAD^+ -hydrolases, e.g. CD38, as well as ADP-ribosyl-acceptor hydrolases (ARHs) that can reverse ADP-ribosylation (Moss et al., 1992, Koch-Nolte et al., 2008).

ADP-ribosylation of surface proteins can be monitored using $^{32}\text{P-NAD}^+$ as substrate (Figure 3.5). Radioactivity incorporated into proteins can be detected by SDS-PAGE autoradiography. ADP-ribosylation attaches a bulky molecule and converts the charge of the target residue.

The first described ADP-ribosyltransferase is diphtheria toxin, which ADP-ribosylates the diphthamide (modified histidine residue) at position 699 of elongation factor 2 and thereby inactivates this essential component of protein biosynthesis and leads to cell death (Honjo et al., 1968). Other bacterial toxins with ADP-ribosyltransferase activity

have since been identified. These include exotoxins A, S and T from *Pseudomonas aeruginosa*, cholera toxin (*Vibrio cholerae*), heat labile enterotoxins (*E.coli*), pertussis toxin (*Bordetella pertussis*), C2 and C3 exotoxins (*Clostridium botulinum*), CDT (*Clostridium difficile*), EDIN (*Staphylococcus aureus*), MTX (*Bacillus sphaericus*) and SpvB (*Salmonella enterica*) which modify intracellular target proteins and thereby inhibit signal transduction or cause cell destruction (Corda and Di Girolamo, 2003, Aktories and Barbieri, 2005, Hottiger et al., 2010)

Toxin-related ADP-ribosyltransferases are also found in vertebrates, either as mono-ADP-ribosyltransferases (ARTs) or poly-ADP-ribosyltransferases (syn.: poly-ADP-ribosylpolymerases, PARPs), which attach multiple ADP-ribose units yielding branched polymers onto acceptor molecules (Hassa and Hottiger, 2008, Koch-Nolte et al., 2008).

ADP-ribosyltransferases can be categorized into two subfamilies, the R-S-E subfamily (ARTC) and the H-Y-E subfamily (ARTD) according to a conserved amino acid motif. The ARTD subfamily encompasses diphtheria toxin, exotoxin A of *Pseudomonas aeruginosa*, cholera toxin secreted by *Vibrio cholerae* and all eukaryotic ARTs catalyzing poly-ADP-ribosylation. In contrast, the ARTC family includes a number of enzymes such as the clostridial C2 and C3 toxins, LT and cholera toxin, SpvB as well as ART2, the ADP-ribosyltransferase responsible for the ADP-ribosylation of CD25. The two subfamilies are distinct in additional secondary structure units (Hottiger et al., 2010).

In mammals, six distinct members of the R-S-E subfamily of ARTs have been cloned to date: ART1, ART2 (ART2.1, ART2.2), ART3 and ART4 which are GPI anchored enzymes, as well as ART5, a soluble enzyme (Glowacki et al., 2001). In humans, only ART1, ART3, ART4 and ART5 are expressed, as the ART2 gene is inactivated by premature stop codons and is thus only a pseudogene (Haag et al., 1994, Glowacki et al., 2002). The mouse has two closely linked copies of the ART2 gene (ART2.1 and ART2.2). Both genes are expressed by immune cells and both gene products - with an approximate 80% amino acid sequence identity - show potent arginine specific ADP-ribosyltransferase activity. The enzymatic activity of ART2.1, which carries an extra disulfide bond (Hong et al., 2009), is regulated by extracellular reducing agents. In contrast to most prokaryotic ARTs, which have only one or a few target proteins, ART1 and ART2 have multiple target proteins - similar to exoS and MTX (Laing et al., 2010).

In mice, ART2.2 is prominently expressed on the cell membrane of naïve T cells and Foxp3⁺CD4⁺CD25⁺ regulatory T cells (Tregs) (Koch-Nolte et al., 1996a, Koch-Nolte et al., 1999, Aswad et al., 2005, Hottiger et al., 2010). ART2.1 is expressed by T cells and by antigen-presenting cells (Koch-Nolte et al., 1995, Hong et al., 2007). The ART2.1 gene is inactivated in B6 mice by a premature stop-codon, i.e. B6 mice express only ART2.2 (Matthes et al., 1997, Kanaitsuka et al., 1997). Conversely, the ART2.2 gene is deleted in NZW (New Zealand white) mice, i.e. these mice express only ART2.1.

Known targets of ART2.2 include the purinoreceptor P2X7 and the integrin LFA-1 (Adriouch et al., 2008, Nemoto et al., 1996, Bannas et al., 2005). P2X7 is expressed on immune cells and acts as a non-selective cation channel (North, 2002, Di Virgilio et al., 2009). In a cascade of events, NAD⁺-dependent ADP-ribosylation of P2X7 causes apoptosis of T cells. This phenomenon, also known as NAD⁺-induced cell death (NICD), is initiated when the P2X7 channel is gated by ADP-ribosylation which induces opening of a non-selective pore causing calcium influx, shedding of CD62L, exposure of phosphatidylserine on the outer leaflet of the plasma membrane, breakdown of the mitochondrial membrane potential, and DNA-fragmentation as a sign of cell death (Seman et al., 2003, Koch-Nolte et al., 2006, Scheuplein et al., 2009).

In this study, HEK-T cells are cotransfected with ART2.2 and CD25 (either wildtype or with mutated arginine residues) in order to identify the target arginines of ART2.2 on CD25 by site-directed mutagenesis and the ³²P-ADP-ribosylation assay illustrated in Figure 3.5. The ART2.2 expressing B6 mice are used for the analysis of CD25 dependent phosphorylation of STAT5. Cells from ART2^{-/-} mice, in which both ART2 genes are inactivated, and cells from P2X7^{-/-} mice, which are resistant to NICD (NAD⁺-induced cell death), are used as controls. ART2^{-/-} mice show a normal development of all major lymphocyte subsets (Ohlrogge et al., 2002). T cells from these mice do not show any detectable cell surface ART activity. ART2^{-/-} T cells show a stronger proliferative response to stimulation with anti-CD3 antibodies than WT controls. Moreover, ART2^{-/-} T cells are resistant to NAD⁺-mediated inhibition of cell proliferation and to NICD (Ohlrogge et al., 2002, Seman et al., 2003).

4 Materials and Methods

4.1 Materials

Laboratory equipment

Product	Product specification	Company
Laboratory Scale	Analytical plus	Ohaus
Autoclave	2540 EK	Tuttnauer
	Varioklav	H& P Labortechnik
Microbiological Incubator	B6060	Heraeus
CO ₂ Incubator	Thermicon T	Heraeus
Cooler	Stratacooler	Stratagene
Thermocycler	Biometra T3	Whatman Biometra, Göttingen
Flow cytometer	FACS Calibur	Becton Dickinson, Heidelberg
Flow cytometer	FACS Canto II	Becton Dickinson, Heidelberg
Electrophoresis System	XCell SureLock Mini- Cell	Invitrogen, Groningen (Netherlands)
Microscope	Neubauer	Zeiss
Microwave	M 637 EC	Miele
Blood counting chamber		Labor Optik
Adjustable volume pipette	Type “research”	Eppendorf
Pipet-Aid	“Express”	BD Biosciences
Table-top processor	Curix60	AGFA
Gel documentation	Edas290 + Camera DC290	Kodak
Thermomixer	Thermomixer compact	Eppendorf
Incubator shaker	Ecotron/Unitron	Infors
Gel system	Perfect Blue Gel System Mini S	PEQLAB Ltd.
Nitrogen tank	K series	Taylor-Wharton
X ray cassettes 18 x 24cm		Dr. Goos-Suprema GmbH
Power supply for agarose gel electrophoresis	Standard power pack P25 BIO1015 LVD	Biometra
Power supply for SDS PAGE	Power Pac 200	BioRAD

and electroblot

Surgical scissors; small,
straight

Aesculap, Tuttlingen

Table centrifuge

5415D

Eppendorf

UV transilluminator

Type T1

Biometra

Vortex mixer genie

Genie 2T

Neolab

Water bath

Type 1007

Society for laboratory
techniques

Centrifuge

Rotanta 460R

Hettich

Consumable supplies

Product

Company

Destaining bags

Amresco

Disposable aspirating pipets

BD Falcon

Disposable syringes

Braun

Fixer

AGFA

Developer

AGFA

5 ml Round-Bottom Tube

Falcon/Becton Dickinson,
Heidelberg, Germany

Hyperfilm ECL

Amersham Biosciences

Needles

Braun

Cryoconservation tubes, 1 ml

Nunc

Cell culture flasks T25, T75

Greiner/Nunc

Cell culture plates (10 cm, 25 cm)

Greiner/Nunc

Gel Blotting paper „GB 003“

Schleicher & Schuell

Kodak Biomax MS X ray film

Kodak Company,
Conneticut, USA

80 µm pore Nitex filter

Cadisch Precision meshes,
London, UK

Nitrocellulose Hybond-C

Schleicher & Schuell

NuPAGE Novex Bis-Tris Gels (10%)

Invitrogen, Groningen,
Netherlands

ImmobilonP (PVDF) transfer membrane

Millipore

Pipette tips

Falcon/BD Biosciences

Safelock tubes

Eppendorf

Dynabeads M-280 Sheep anti mouse IgG1

Invitrogen

Dynabeads M-450 sheep anti rat	Dynal, Hamburg
Polypropylene tubes, sterile (15 ml)	Greiner
Filtration devices (Steriflip, Stericup)	Millipore, Billerica, USA
TruCount Tubes	BD
Medical Hygienic Gloves „Safeskin“	Hartmann, Heidenheim
96 well microtiter plate V bottom/ U bottom/flat bottom	Nunc
24 well microtiter plate	Nunc
6 well microtiter plate	Nunc
Centrifuge tubes, 15 ml/50 ml sterile	Falcon/BD Biosciences

Mice

P2X7^{-/-} mice, kindly provided by Chris Gabel, Pfizer, Ann Arbor, MI (Solle et al., 2001) and ART2^{-/-} mice, generated in the Koch-Nolte lab, Hamburg (Ohlrogge et al., 2002) were backcrossed onto the B6 background for 12 generations and were maintained under specific pathogen-free conditions at the central animal facility of the UKE. DEREK (B6) mice expressing DTR-eGFP, kindly provided by Tim Sparwasser, Helmholtz Zentrum für Infektionsforschung, Hannover, under the control of the Foxp3 promoter (Lahl et al., 2007) were backcrossed onto P2X7^{-/-} or ART2^{-/-} backgrounds.

Cell lines

YAC-1 lymphoma cells, kindly provided by Jürgen Löhler, Heinrich Pette Institute, Hamburg, were cultured in RPMI-1640 supplemented with 10% FCS, 2 mM glutamine, 2 mM sodium pyruvate (complete RPMI).

CTLL-2 cells, kindly provided by Marc Pallardy, INSERM U 461, Châtenay-Malabry, were maintained in complete RPMI supplemented with 10 ng/ml human recombinant IL-2 (10000 U/ml, Roche) and 0.0001% 2-mercaptoethanol. CTLL-2 cells were stably transfected with an expression construct for ART2.2 (pME.CD8LF-ART2.2) (Koch-Nolte et al., 1999).

HEK-T cells: human embryonic kidney cells; ATCC number: CRL-1573

Bacteria

XL 10-Gold Ultracompetent Cells (Stratagene, Amsterdam, Netherlands)

Antibodies/Streptavidin conjugates

Antibody	Clone	Company
anti human Stat5 IgG1, Alexa Fluor® 647 Mouse	pY649	BD biosciences, Heidelberg, Germany
Rat anti mouse ART2.2, IgG2a, P649	R8A9	AG Nolte, Hamburg,

	NIKA	Germany
Rabbit anti mouse/anti human CD25	polyclonal	Abcam, Cambridge, UK
Rat anti mouse CD25, IgG1	PC 61	BD biosciences, Heidelberg, Germany
Rat anti mouse ART2.2	K12760	AG Nolte, Hamburg, Germany
Rat anti mouse CD25, IgG1, APC	PC61.5	eBioscience, Frankfurt, Germany
Mouse anti human CD25, IgG1, APC	M-A251	BD biosciences, Heidelberg, Germany
Rat anti mouse CD4, IgG2a, APC	L3T4	BD biosciences, Heidelberg, Germany
Streptavidin, APC		BD biosciences, Heidelberg, Germany
Streptavidin, FITC		GE Healthcare, Munich, Germany
Streptavidin, PE		BD biosciences, Heidelberg, Germany
Rat anti mouse CD4, IgG2a, V450	L3T4	BD Horizon, Heidelberg, Germany
Rabbit anti mouse P2X7, polyclonal, AF647	K1G	AG Nolte, Hamburg, Germany

Chemicals

Product	Company
ADPR	Sigma Aldrich, Munich, Germany
AEBSF	MP Biomedicals
Beta mercaptoethanol (50 mM)	Gibco
Aqua ad iniectabilia	Braun
BSA	PAA
³² P-NAD ⁺ , 10 mCi/ml	PerkinElmer
Carbenicillin	Serva, Heidelberg, Germany
Coloidal blue staining kit	Invitrogen, Groningen, Netherlands
DMSO, Dimethyl sulfoxide	Sigma
DNA typing grade agarose	Gibco
DNA loading Dye 6x	MBI Fermentas

dNTPs (10 mM)	Invitrogen
ECL Western blotting detection reagent	Amersham Biosciences
Ethanol, dried	Merck
Ethidium bromide	Molecular probes
Gel-Dry™ Drying solution	Invitrogen
GeneRuler™ 1kb DNA Ladder	MBI Fermentas
HEPES (1 M)	Gibco
Human interleukin-2 (10.000 U/ml)	Roche
Mouse interleukin-2 (10 U/ng, 0,5 µg/µl)	eBioscience
Novex Sharp Pre-stained protein standard	MBI Fermentas
Novex Colloidal Blue staining kit	Invitrogen
NAD ⁺	Sigma
Kaleidoscope™ Precision	Bio-Rad, Munich, Germany
NuPAGE Antioxidant Invitrogen,	Groningen (Niederlande)
NuPAGE LDS sample buffer 4x	Invitrogen, Groningen (Niederlande)
NuPAGE sample reducing agent 10x (DTT)	Invitrogen, Groningen (Niederlande)
NuPAGE SDS-PAGE MES running buffer	Invitrogen, Groningen (Niederlande)
NuPAGE SDS-PAGE MOPS running buffer	Invitrogen, Groningen (Niederlande)
NuPAGE SDS-PAGE transfer buffer	Invitrogen, Groningen (Niederlande)
Propidium iodide	BD Biosciences
Protein G Sepharose (50%)	Amersham Biosciences
Paraformaldehyde	Merck
M2 Sepharose (50%)	Sigma
20 x TAE-Puffer	Gibco BRL, Eggenstein
Milk powder	Carl Roth
Methanol	Walter GmbH
TAE Buffer (Tris acetate EDTA buffer) (50x)	Gibco
Triton X 100	Sigma
Tween20	ICI Americas

PBS	Gibco
Dulbecco's modified Eagle medium (DMEM)	Invitrogen, Groningen, Netherlands
Fetal calf serum	Biochrom, Berlin
G418	Gibco
Gentamicin 50 mg/dl	Gibco BRL, Karlsruhe
JetPEI Transfection reagent	Polyplus, New York, USA
L-Glutamin, 200 mM	Gibco BRL, Karlsruhe
Sodium pyruvate, 100 mM	Gibco BRL, Karlsruhe
Non-essential amino acids, 100x	Gibco BRL, Karlsruhe
Isotonic sodium chloride solution, 154 mM NaCl	Braun

Enzymes

Enzyme	Company
DNA Polymerase	Roche (2.500 U/ml)
SuperScript II Reverse Transcriptase	Invitrogen, Karlsruhe, Germany
PFU-Turbo DNA Polymerase	Stratagene, Amsterdam, Netherlands
T4 Ligase	Invitrogen, Karlsruhe, Germany
Restriction enzyme Not I (20.000 U/ml)	New England Biolabs, Frankfurt, Germany
Restriction enzyme Eco RI (20.000 U/ml)	New England Biolabs, Frankfurt, Germany
NEB buffer 3	New England Biolabs

Primer

Designed with DNA Star software (Madison, USA) and ordered from Metabion (Martinsried, Germany). The numbers indicate the mutation site and the letter the orientation of the primer (F=forward; R=reverse).

Name

hCD25 (R35,36K)-F	GCAAGAGAGGTTTC AAAA AACTAAAGGAATTGG
hCD25 (R35,36K)-R	CCAATTCCTTTAGTTTT TTT TGAAACCTCTCTTGC

Vectors

The cDNA expression vectors encoding mouse and human CD25 (pCMVSPORT6), ART2.2 (pME.CD8F-ART2.2), and nuclear GFP (pEGFP-LKLF, encoding a fusion protein of GFP and the transactivating domain of the LKLF transcription factor) were cloned previously in the lab (Hann, 2008, Möller et al., 2007, Koch-Nolte et al., 1999).

A plasmid encoding the RallK mutant of human CD25, in which all eleven arginines are mutated to lysins, was purchased from Genieart (Regensburg, Germany).

Mutants were generated by PCR as described below.

Cell culture media and solutions:

Components added to cell culture media underwent sterile filtration (pores 0,22 µM). Complement factors contained in the fetal calf serum were inactivated at 56°C for 30 minutes.

Cell culture media

RPMI complete medium	1640 RPMI (Roswell Park Memorial Institute), 10% FCS, 2 mM L-glutamine, 1mM sodium pyruvate
----------------------	---

RPMI (+IL-2) complete medium	1640 RPMI, 10% FCS, 2 mM L-glutamine, 1mM sodium pyruvate, 10 U/ml IL-2, 50 µM 2-mercaptoethanol
------------------------------	--

DMEM complete medium	DMEM, 10% FCS, 2 mM L-Glutamin, 1 mM sodium pyruvate, 1x non-essential amino acids, 10 mM HEPES buffer
----------------------	--

Cell culture freezing medium for suspension cells	RPMI, 20% FCS, 10% DMSO
---	-------------------------

Cell culture freezing medium for adherent cells	DMEM, 20% FCS, 10% DMSO
---	-------------------------

Media for bacterial cultures

LB Agar (Miller)	1,5% Agar, 1% casein, 0,5% yeast extract, 0,05% NaCl (Difco/Becton Dickinson)
------------------	---

LB Medium (Miller)	1 % Pepton, 1 % NaCl, 0,5 % yeast extract (Invitrogen)
--------------------	--

SOC Medium	2 % trypton, 0,5 % yeast extract, 8,6 mM NaCl, 2,5 mM KCl, 20 mM MgSO ₄ , 20 mM Glucose (Gibco)
Cell lysis buffer	
Lysis buffer for radioactive assay	1 % TritonX100, 1 mM AEBSF, 1 mM ADP Ribose, 100 μM NAD ⁺ , 2 mM EDTA in PBS
Ack lysis buffer for erythrocytolysis	8.29g NH ₄ Cl, 1g KHCO ₃ , 0.037g EDTA ad 1L with ddH ₂ O
SDS-Page and Western blots	
Antibody buffer	1x TBS 0,05% Tween-20, 5% milk powder
Blocking buffer	1x TBS, 5% milk powder
Blot buffer	10% methanol, 0,1% antioxidant, 5% transfer buffer
MES running buffer	50 mM MES, 50 mM TRIS-Base, 3,5 mM SDS, 1 mM EDTA, pH 7,3 (NuPage, Invitrogen)
MOPS running buffer	50 mM MOPS, 1 M TRIS-Base, 3,5 mM SDS, 12 mM EDTA: pH 7,7 (NuPAGE Invitrogen)
SDS loading buffer	NuPage SDS sample buffer 1x, NuPage sample reducing agent 1x (1 mM DTT) in H ₂ O
Transfer buffer (20x)	0,5 M Bicin, 0,5 M BIS-TRIS, 20,5 mM EDTA, 1mM Chlorobutanol
TBS	0,025 M Tris-HCl, pH 7,4, 0,15 M NaCl
Washing buffer	1x TBS, 0,05% Tween-20

Kits

Gel extraction kit	QIAquick Gel Extraction Kit, Qiagen, Hilden
Antibody immunoprecipitation matrix	Biotechnology, Rockford (USA)
Endofree plasmid preparation	QIAprep Spin Miniprep Kit, Qiagen, Hilden Endofree Plasmid Maxi kit, Qiagen
Treg isolation kit	CD4 ⁺ CD25 ⁺ Regulatory T Cell Isolation Kit (mouse), Miltenyi Biotec, Bergisch Gladbach, Germany
Human interleukin-2 Biotin Conjugate	Fluorokine, R&D Systems

4.2 Methods

4.2.1 Cell biology methods

Cell culture

YAC-1 lymphoma cells, kindly provided by Jürgen Löhler, Heinrich Pette Institute, Hamburg, were cultured in RPMI-1640 supplemented with 10% FCS, 2 mM glutamine, 2 mM sodium pyruvate (complete RPMI). The YAC-1 line was created by inoculation of a newborn A/sn-Mouse with the Maloney leukemia virus-1 (Kiessling et al., 1975). The cell-line was sorted three times for high level of cell surface ART activity following incubation of cells with etheno-NAD⁺ and selection of cells showing high staining with the etheno-adenosine-specific 1G4 monoclonal antibody (Krebs et al., 2003).

CTLL-2 cells, kindly provided by Marc Pallardy, INSERM U 461, Châtenay- Malabry, were maintained in complete RPMI supplemented with 10 ng/ml human recombinant IL-2 (10000 U/ml, Roche) and 0.0001% 2 mercaptoethanol. CTLL-2 cells were stably transfected with an expression construct for ART2.2 (pME.CD8LFART2.2) and regularly supplemented with Genitacin (G418, 1 µg/ml) for the selection of transfected cells.

The adherent human embryonic kidney cell line (HEK-T) was harvested by discarding the medium, washing with PBS^{-/-} and an incubation step with 1 ml PBS supplemented with 1% Trypsin at 37°C for three to four minutes.

Isolation of mouse regulatory T cells

Spleen cells were prepared from 16-week old mice and filtered through a 70 µm cell strainer into a 50 ml falcon tube. After erythrocyte lysis with Ack lysis buffer, B cells were depleted with 100 µl Dynabead-conjugated sheep anti-mouse IgG (M-280, Invitrogen). In order to deplete any remaining B cells as well as CD8⁺ T cells, the cell suspension was incubated with 12 µl anti-ms-CD8a and anti-msCD19 antibody for 20-30 minutes at 4°C. Cells that had bound to the antibodies were eliminated by incubation with 100 µl anti-rat IgG Dynabeads (Invitrogen, M-450).

Tregs were positively selected by magnetic cell sorting using PE conjugated anti-CD25 and magnetic bead conjugated anti-PE antibody according to the manufacturer's instructions (Miltenyi Biotec, Figure 3.1). After a centrifugation step, the cells were resuspended in 50 µl MACS buffer (PBS 0,2% BSA 2 mM EDTA, Gentamycin 10 µl/ml). For the isolation of regulatory T cells, the cell suspension was incubated with 10 µl anti-mouse-CD25 PE microbeads (kit) for 15 minutes at 4°C, then 10 µl anti-PE microbeads for 15 minutes at 4°C. After two washing steps, the cells were loaded onto a magnetic cell separator. The flow-through was collected and the column washed twice with 1 ml of MACS buffer. The CD25⁺ T cells bound to the column were then eluted by the addition of MACS buffer using a plunger. Cell numbers were determined by counting in a Neubauer chamber. Purity, determined by flow cytometry, was > 90%.

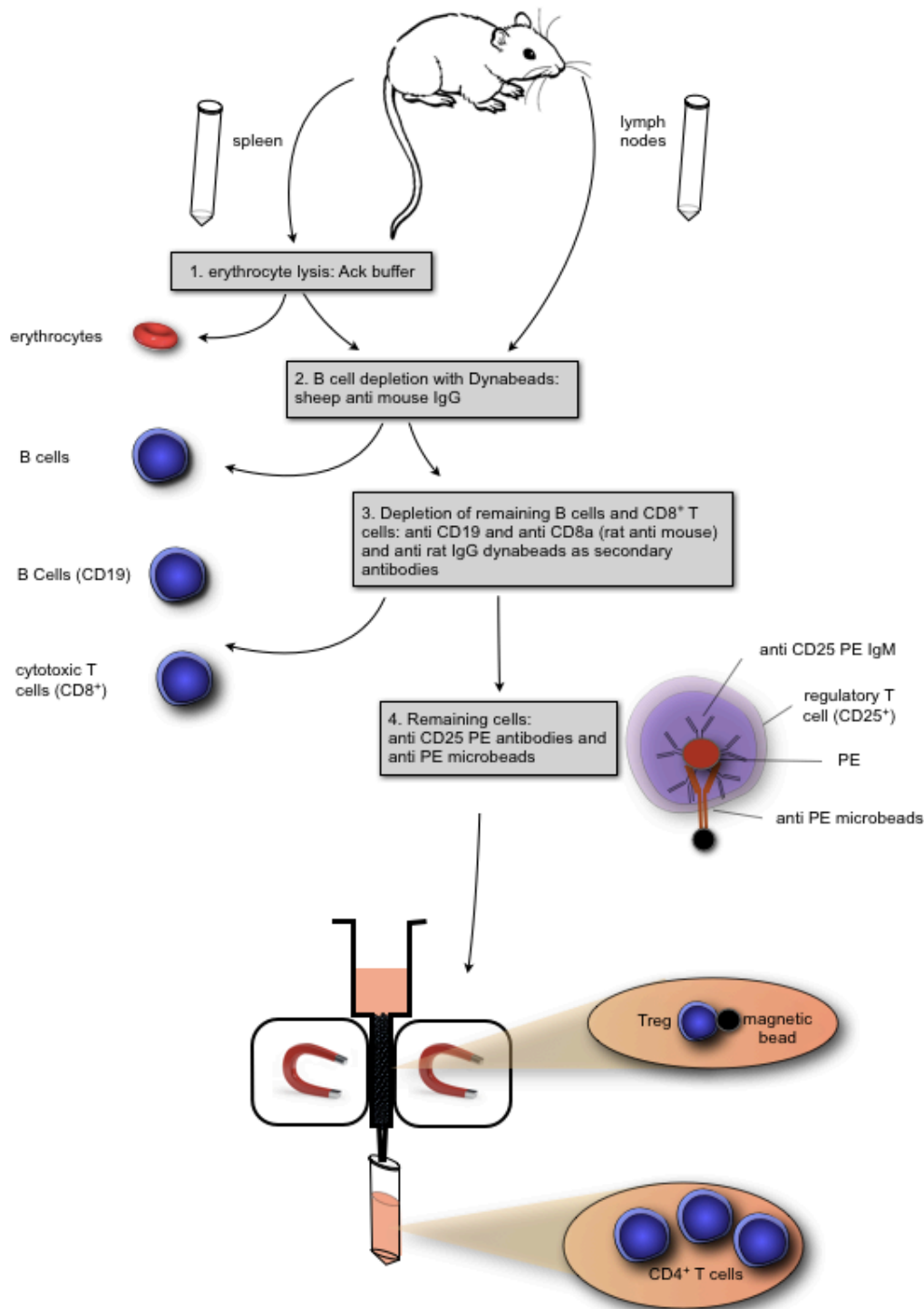


Figure 4.1: Lymph node isolation and purification of Tregs with the miltenyi kit. In a first step, spleen and lymph nodes are isolated from the mouse. Spleen cells are incubated with Ack buffer, which causes erythrocyte lysis. Cells are then incubated with anti IgG Dynabeads (Invitrogen) in order to deplete B cells. The remaining cells are incubated with rat anti-mouse CD8a and CD19 antibodies in order to deplete cytotoxic T cells as well as monocytes/macrophages with sheep anti rat IgG Dynabeads (Invitrogen). Tregs are then labeled with a PE-conjugated anti CD25 antibody (7D4, IgM), which is then used for attaching magnetic microbeads coated with anti-PE. By placing the cell solution in a magnetic column, CD25 positive cells are retained in the magnetic field of the column, while the flow-through contains the pre-enriched CD4⁺ T cells. Removing the column from the magnetic field then allows elution of the Tregs (coated with PE-conjugated anti-CD25 and anti-PE microbeads).

Cell proliferation assay

In order to assess the proliferation of CTLL-2 cells (untransfected and stably transfected with ART2.2) under various conditions, the cells were first depleted of IL-2 contained in the medium by washing them twice with culture medium, followed by an incubation in culture medium without IL-2 over night. Cells were seeded in a 24-well plate (3×10^4 cells per well) and cultivated in medium containing serial dilutions of human IL-2 (Roche). Medium containing or lacking NAD^+ (final concentration $100 \mu\text{M}$) was added every 12 hours. Cell numbers were determined after five days by flow cytometry using Trucount™ Control beads (BD).

4.2.2 Immunological methods

Flow cytometry

Fluorochrome-conjugated mAbs were used against mouse CD25 (PC61, BD; 7D4, Miltenyi) human CD25 (M-A251, BD), ART2.2 (Nika 102, Institute of Immunology, Koch-Nolte et al., 1999), and pSTAT5 (47, BD). 1×10^6 cells were suspended in $100 \mu\text{l}$ DPBS (Phosphat Buffered Saline; GIBCO) in a 5 ml Falcon tube. Antibodies were used at a dilution of 1:100 – 1:200 and incubation time of 20 minutes at 4°C . The cell suspension underwent washing twice with 1 ml of RPMI complete medium and centrifugation at 1600 rpm for 5 minutes. Stained cells were measured on a FACS Calibur (BD) and analyzed using FlowJo software (TriStar).

STAT5 phosphorylation assay

For the detection of phosphorylated STAT5 (residue Y694), purified Tregs (1×10^5 cells/ $100 \mu\text{l}$) were incubated in the absence or presence of $30 \mu\text{M}$ NAD^+ for 15 minutes at 4°C before the addition of 20 U/ml mouse IL-2 (eBioscience) and further incubation for 15 minutes at 37°C . The cells were then fixed in 2% PFA for 10 minutes at 37°C and 90% methanol at -20°C . Cells were stained with APC-conjugated anti-phospho-STAT5 according to the manufacturer's instructions (BD).

Interleukin-2 binding assay

1×10^5 cells were incubated with 30 ng biotinylated human IL-2 (R&D Systems, $3 \mu\text{g/ml}$) or 50 ng soybean-trypsin inhibitor (R&D Systems, $10 \mu\text{g/ml}$) for 60 min at 4°C before addition of $0,2 \mu\text{g/ml}$ APC-conjugated streptavidin (BD) (Figure 4.2). Parallel aliquots of cells were preincubated with or without unlabeled mouse IL-2 ($50 \mu\text{g/ml}$, eBioscience) or $50 \mu\text{M}$ NAD^+ .

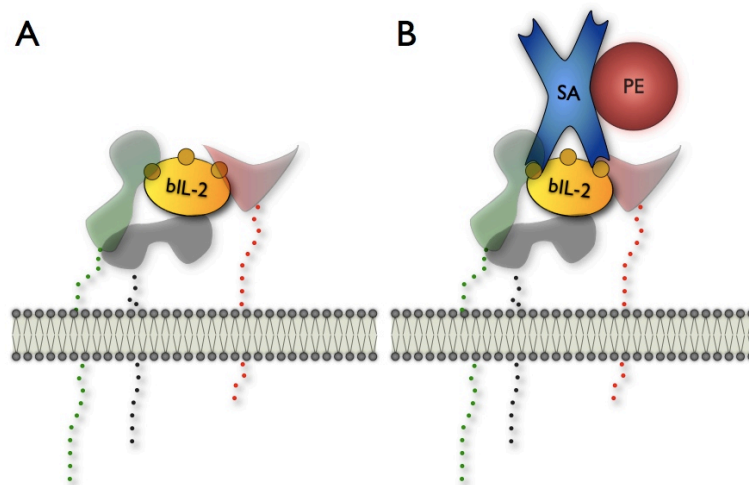


Figure 4.2: Schematic diagram of IL-2 binding assay. A: biotinylated IL-2 bound to the heterotrimeric IL-2R. B: in a second step, the biotin molecules are detected by streptavidin, which is conjugated with PE. Thus, detection of IL-2 with flow cytometry is made possible.

4.2.3 Protein biochemistry methods

ADP-ribosylation assay with [³²P]-NAD⁺

Transiently transfected HEK-T cells were cultured in a 6-well plate precoated with poly-L-lysine. 48 hours post transfection, the culture medium was removed and the adherent cells were gently washed with prewarmed serum-free X vivo medium (Bio Whittaker) and then incubated in serum-free X vivo medium containing [³²P]-NAD⁺ (2,5 µCi, 0,4 µM) (PerkinElmer) for 20 minutes at 37°C. Cells were gently washed with prewarmed X vivo medium and then lysed in PBS, 1% Triton-X100, 1 mM AEBSF (Sigma) for 20 min at 4°C. Insoluble material was pelleted by high-speed centrifugation (15 min 13.000 g) and soluble proteins in total cell lysates were size fractionated on precast SDS-PAGE gels (Invitrogen) (1 x 10⁵ cell equivalents/lane). Prior to injecting the samples into the wells, 20 µl cell lysate was inactivated with 5 µl NuPAGE LDS 4x buffer (Invitrogen) and 2,5 µl DTT at 70°C for 10-15 minutes. The gel ran for 45 minutes at 200 V, 100 mA in a chamber filled with MES buffer (Invitrogen) (Figure 4.3).

Total proteins were detected by Coomassie staining of the gels (20 ml methanol, 55 ml distilled water, 20 ml stainer A and 5 ml stainer B from the Colloidal Blue Staining kit, Invitrogen). Excess stain was removed by incubation in distilled water and destaining bags containing activated carbon (Amresco) over night. For detection of radiolabeled proteins, the gel was exposed to an X-ray film at -80°C for 18 – 72 hours.

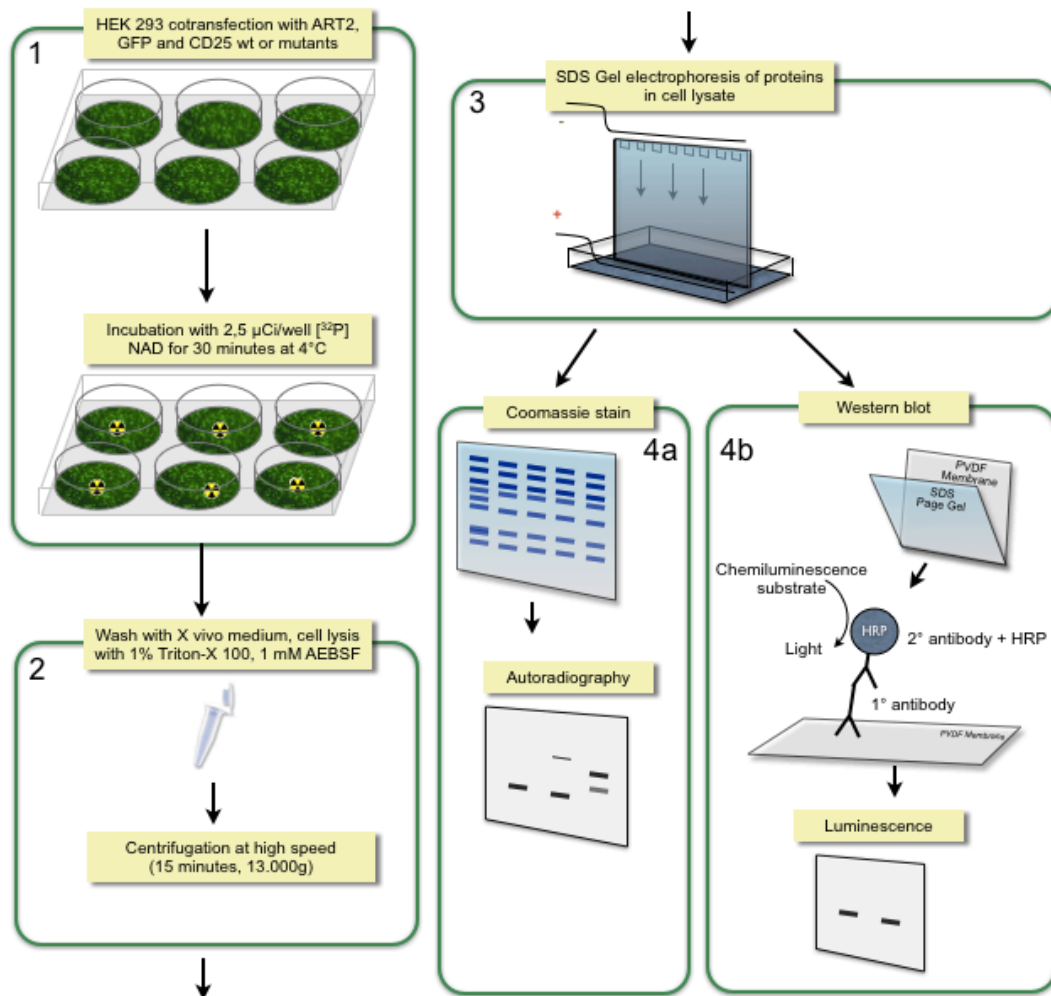


Figure 4.3: Schematic diagram of the assay for radioactive labeling and detection of ADP-ribosylated proteins. Transfected HEK-T cells were incubated with radioactive [^{32}P]-NAD $^{+}$ (1), washed and lysed with PBS (1% Triton-X 100, 1 mM AEBSF). Nuclei were pelleted by centrifugation at high speed (2) and soluble proteins were size-fractionated by SDS-PAGE gel electrophoresis (3). Proteins were stained by Coomassie or blotted onto a PDVF membrane for Western blot analysis. Here, a primary antibody detects the target protein, for example CD25, while a secondary antibody conjugated with an enzyme (horse raddish protein, HRP) binds to the first antibody. This enzyme then produces a signal once exposed to a chemiluminescence substrate (4b). Radiolabeled proteins were detected by autoradiography, placing either the dried gel or the blot into a cassette containing an X-ray film (4a, b)

Immunoprecipitation

In order to specifically isolate CD25 from the cell lysate, an immunoprecipitation was performed with an anti CD25 antibody (PC61) coupled to an aminolink matrix according to the manufacturer's instructions (Pierce). After incubation with cell lysates for 60 minutes at 4°C, beads were washed with PBS, 1% Triton-X 100, and non-covalently bound proteins were eluted from the matrix by incubation in SDS-PAGE sample buffer for 10 minutes at 70°C and centrifugation at 13000 rpm for 1 minute. The eluted protein is then contained in the supernatant.

Western Blot

For immunodetection of CD25, proteins were blotted from the gels onto PVDF membranes. The PVDF membrane was activated with methanol. The blot ran for 90 minutes at 100 V and 300 mA in a chamber stacked with sponges soaked in blotting buffer, filter paper and the PVDF membrane on the gel.

In order to prevent binding of the antibody to the membrane, the PVDF membrane was blocked with TBS containing 5% milk powder for 20 minutes at room temperature. The membrane was washed twice with a solution containing 0,05% Tween-20. CD25 was detected with a polyclonal rabbit anti-CD25 antibody (1:1000 in TBS containing 5% milk powder, 0,01% Tween-20 and 0,1% sodium azide) for 60 minutes at 4°C (abcam) and PO-conjugated anti-rabbit IgG (1:5000 in TBS, 5% milk powder, 0,01% Tween 20 and 0,1% sodium azide) at 4°C for one hour using the ECL-system (Amersham). For this purpose, the membrane was incubated with 2 ml reagent A and B (ECL Western blotting detection reagents and analysis system kit) for 2 minutes. The membrane was wrapped in a cling film and put into an ECL film cassette with an ECL film (Amersham). The film was exposed for 30 seconds, 2 minutes and 20 minutes. In order to detect radiolabeled proteins, gels and blots were exposed to an X-ray film at -80°C for 18 – 72 hours.

4.2.4 Molecular biology techniques

Site-directed mutagenesis

A synthetic cDNA clone encoding human CD25 in which all extracellular arginine residues were replaced by lysine, designated RallK, was purchased from GeneArt (Invitrogen).

The coding region for human CD25 was PCR amplified from activated PBLs and cloned into the pCMV-Sport6 vector (Invitrogen) (Hann, 2008). Arginine residues were substituted with lysine (and lysine with arginine in case of the RallK variant of human CD25) using site-directed mutagenesis. For this purpose, 5 ng of the CD25 plasmid (dsDNA), 125 pmol/μl forward and reverse oligonucleotide primers containing the desired mutation (designed with DNA Star software, see Materials section), 1 μl desoxynucleoside triphosphates (dNTPs), 5 μl 10 x Pfu Buffer, 1 μl Pfu Turbo Polymerase (Stratagene) and HPLC water were mixed in a PCR tube in order to obtain a final volume of 50 μl. Next, a PCR amplification was performed, consisting of a series of cycles:

Step	Temperature [°C]	Length	Repeats
Initialization step	95	30 sec	-
Denaturation step	95	30 min	x 29
Annealing step	55	30 sec	
Elongation step	68	7 min	
Final elongation step	68	10 min	-
Final hold	4	∞	-

In order to eliminate native unchanged plasmid, the restriction enzyme DpnI was used (target sequence: 5'-Gm6ATC-3'), which only digests methylated DNA. 15 µl Plasmid DNA were incubated with 3 µl 6x DPN I for one hour at 37°C. The DNA was transformed into ultracompetent XL-10 *E. coli* (Stratagene); plasmids were prepared from single colonies and checked for mutagenesis by DNA-sequencing as described below.

Gel electrophoresis

For the size-fractioning of digested DNA fragments, 3 µl 6x DNA Loading Dye (MBI Fermentas) was added to 15 µl of DNA and loaded onto an agarose gel (TAE, 1% agarose, 0,1 µg/ml ethidium bromide). Ethidium bromide is an intercalating agent that increases fluorescence intensity and thus makes the DNA visible when exposed to ultraviolet light (250-310 nm). 3 µl of the 1kb DNA Ladder (750 ng per slot, Gene Ruler, MBI Fermentas) were used as a molecular weight marker. The chamber was then connected to a power source and ran for approximately 45 minutes with 100 V current.

Extraction of DNA from agarose gels

DNA bands were visualized using ultraviolet light, excised from the gel with a spatula and then purified with a gel extraction kit (Qiagen). The gel slices were dissolved in a buffer containing a saline solution and then applied to a spin column. The nucleic acid adsorbs to the membrane and impurities are washed away (salt, enzymes, gel residues, nucleotides). The DNA was eluted from the column with distilled water.

Digestion of DNA fragments with restriction enzymes

A synthetic cDNA encoding human CD25 in which all 11 arginine residues were replaced by lysine, was purchased from Genentech and cloned into the pCMV-Sport6 and pcDNA6 vectors (Figure 4.4). For this purpose, the pMA plasmid containing the hCD25 insert and the plasmid containing the pCMVSPORT6 vector and the pcDNA6 vector were digested with the restriction enzymes *Eco* R1 and *Not* 1. The enzymes cause the formation of “sticky ends”.

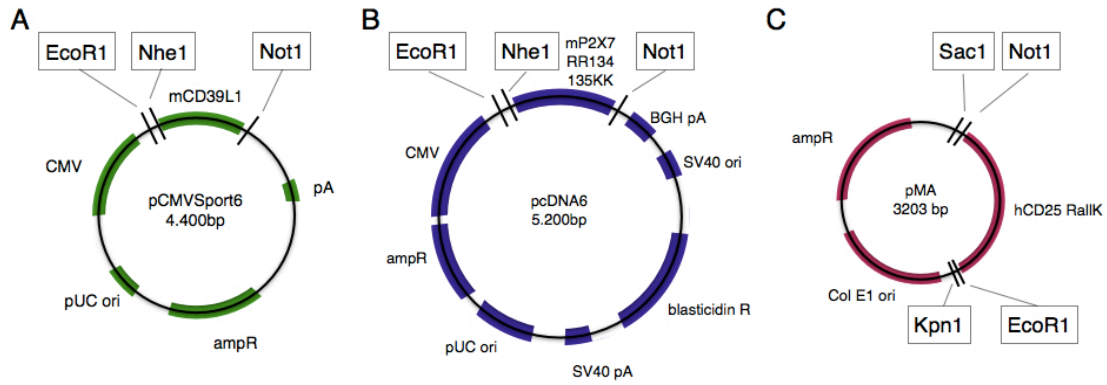


Figure 4.4: Plasmids used for cloning. A: pCMVSPORT6 vector, used for transient transfection of HEK-T cells. For cloning purposes, the pCMV Sport6 vector containing a mCD39L1 insert was used, which has a DNA length of 1600 bp. B: pcDNA6 vector, used for stable transfection of cell culture cells. Here, the plasmid contains an mP2X7 insert with a DNA length of 1800 bp. C: plasmid containing the coding region for human CD25 protein in which all arginines are mutated to lysine (RallK). Subsequently, the CD25 insert was cloned into the pCMVSPORT6 and pcDNA6 vector.

2 µg plasmid DNA were incubated with 2 µl BSA (10x), 2 µl NEB3 buffer, 1 µl Eco R1 and 1 µl Not 1 and distilled water (filling up to 20 µl) for 3 hours at 37°C, another 20 minutes at 65°C to stop the reaction and then at 4°C in order to cool down.

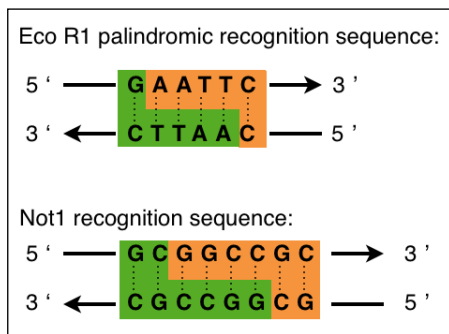


Figure 4.5: Recognition sites of the restriction enzymes EcoR1 and Not1

Ligation of DNA fragments

The amount of vector and insert were estimated on agarose gels (ethidium bromide staining) and then ligated at a molar ratio of 1 to 2 (vector to insert). 4 µl 5x T4 buffer, 1 µl T4 ligase (Invitrogen), the required amount of DNA were mixed and the volume was adjusted with distilled water to 20 µl. As a relegation control, water was added instead of the insert to the vector. The mixture was incubated at 14°C for 15 hours. Ligations were transformed into ultracompetent E.coli and plasmids were prepared from individual colonies as described below. Plasmids were then digested with Eco R1 and Not 1 in order to verify the correct ligation (

Figure 4.6).

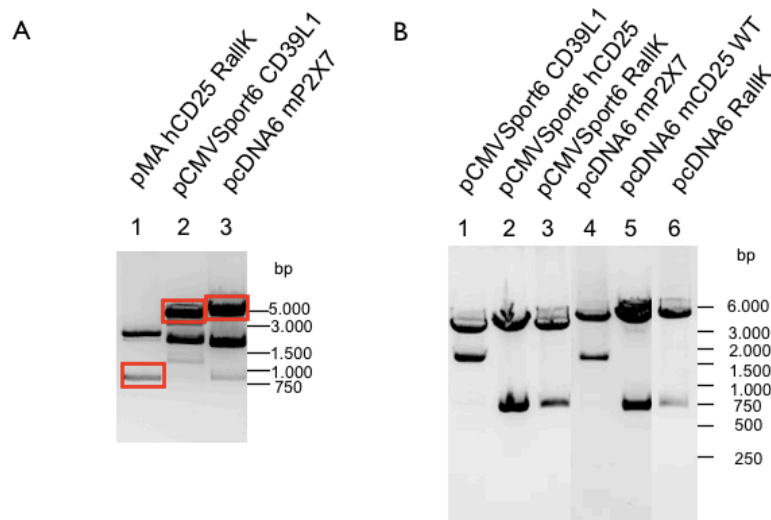


Figure 4.6: Cloning of hCD25 RallK into pCMV Sport6 and pcDNA6. Plasmids were digested with the restriction enzymes *NotI* and *EcoRI* for 3 hours at 37°C, followed by 20 minutes at 65°C. Digested DNA was then transferred to an agarose gel for size fractionation. A: Digested DNA from the three plasmids before cloning. The bands that were recovered for cloning are marked with red boxes. B: Digested DNA after cloning the hCD25 RallK fragment into the pCMV Sport6 and pcDNA6 vector.

Transformation of ultracompetent XL Gold *E.coli* cells

In order to increase the amount of plasmid DNA, 60 µl ultracompetent XL Gold *E.coli* (Stategene) cells were transfected with 1 µl undiluted CD25 plasmid (wild type or mutants) in a polypropylene tube. The mixture was incubated for 30 minutes at 4°C in order to let the DNA attach to the bacterial membrane. The tube was exposed to a 42°C heat shock in the water bath in which the bacterial membrane becomes permeable for the DNA. The reaction was stopped with a 2 minute incubation on ice and then incubated for an hour with 450 µl SOC medium at 37°C. The cells were plated on LB agar dishes (100 µg/ml carbenicillin, selection of ampicillin resistant bacteria) for 15 hours at 37°C, 5% CO₂. Four colonies were picked from each plate on the following day and transferred to LBS liquid medium and again incubated at 37°C overnight.

Minipreparation of plasmid DNA

The DNA contained in the bacterial cultures was purified using the original mini prep Qiagen reagents. The preparation was done according to the protocol, i.e. after centrifugation of the bacterial cell suspension at 4000 g for 10 minutes, the DNA-containing pellets were diluted in several buffers containing NaOH, SDS and RNases, thus denatured and precipitated with a buffer containing large amounts of salt. The DNA was then loaded onto a silica matrix that bound the DNA. Several washing buffers removed proteins and, eventually, the DNA plasmid was eluted with an elution buffer. DNA concentration was determined with a Nanodrop instrument (Peqlab). Sequence analysis was done by SeqLab (Göttingen, Germany) and the results were analyzed with the SeqMan software (DNA star) (Figure 4.7).

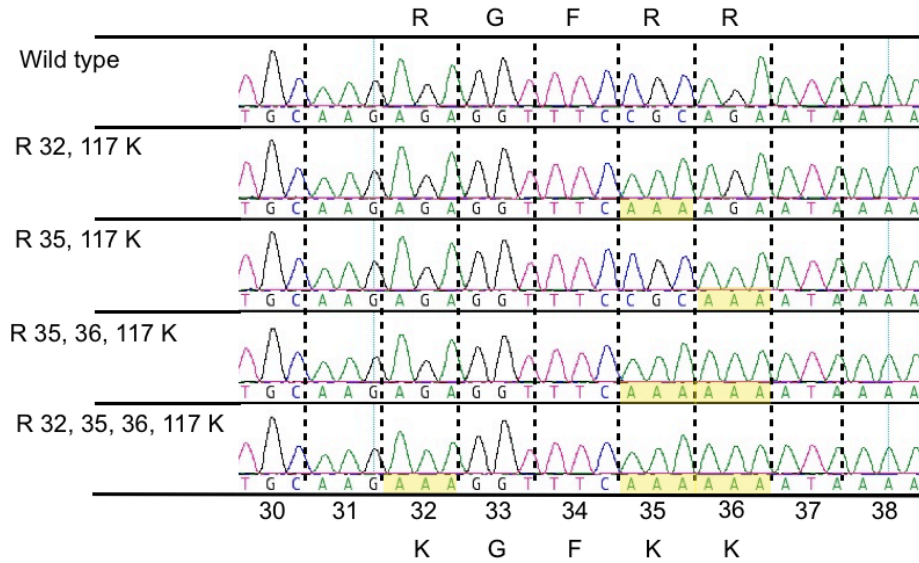


Figure 4.7: Site-directed mutagenesis of CD25. The image shows the sequences of the wild type human CD25 and of four different mutants from codons number 30 to 38. Arginines (CGC/AGA), which were mutated into lysins (AAA) are marked in yellow.

Transient transfection of HEK-T cells

In order to analyze the differences between wildtype and mutant CD25, the expression constructs (5 μg per 10^6 cells) were transfected into HEK-T cells with the jetPEI transfection reagent (Polyplus).

In order to do so, HEK-T cells were harvested by trypsinization from a T75 cell flask (60-70% confluent, freshly passaged on the previous day) washed in medium containing 10% SOC and then resuspended in 25 ml medium. 2 ml were used for each transfection. 4 μg of the human wildtype or mutant CD25, 0,5 μg murine ART2.2 and 0,5 μg GFP were diluted in 250 μl NaCl. 10 μl JetPEI reagent, also diluted in 250 μl NaCl, was added to each DNA solution and incubated for 30 minutes at room temperature. Then, the Jet Pei mixture was dripped onto the cell suspension. After another 15 minutes at room temperature, the cell suspension was transferred onto two 6-well cell culture plates, one for expression analysis and the other one for radioactive labeling.

5 Results

This thesis analyzes the structural and functional aspects of ADP-ribosylation of CD25 by ART2.2. The results are divided into three sections. The first section shows that CD25 is, among other proteins, a target of ART2.2. The experiments illustrated in the second section analyze the functional consequences of ADP-ribosylation of CD25 as part of the heterotrimeric IL-2R on lymphoma cells and primary T cells. Results from IL-2 dependent cell proliferation assays, IL-2 binding assays, and IL-2 induced phosphorylation of STAT5 are presented. In the last section, potential target arginines of ART2.2 on CD25 are identified by mutational analyses.

5.1 CD25 is a main target of ADP-ribosyltransferase 2 (ART2) on Yac-1 cells

Known ART2.2 targets include the purinoreceptor P2X7 and LFA-1 (Seman et al., 2003, Nemoto et al., 1996). The Yac-1 lymphoma cell line constitutively expresses low levels of ART2.2 and high levels of CD25 (Figure 5.1A). In a previous study, affinity purification of etheno-ADP-ribosylated proteins from Yac-1 cells followed by mass spectrometry analyses had identified a band of 55kDa as CD25 (Hann, 2008).

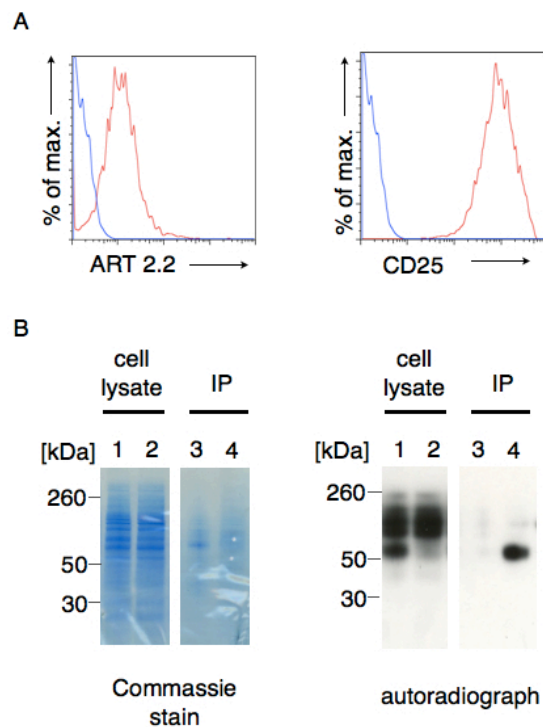


Figure 5.1: Identification of CD25 as a major ADP-ribosylation target on Yac-1 lymphoma cells.

A) YAC-1 cells were stained with Alexa647-conjugated antibodies against ART2.2 (NikaA9), CD25 (PC61) and bound antibodies were detected by flow cytometry (red histograms; unstained cells: blue histograms). YAC-1 cells were incubated with [32 P]-NAD $^{+}$ (2,5 μ Ci/well) for 20 minutes at 37°C, then washed and lysed for 20 minutes with 1% Triton-X 100/PBS. After centrifugation of the nuclei and other insoluble fragments, immunoprecipitations were performed with bead-immobilized α -CD25 (lane 4) and control beads (lane 3). The proteins of the whole cell lysates (lane 1 and 2) and the immunoprecipitated proteins (lane 3 and 4) were separated with gel electrophoresis. Proteins were stained with Coomassie and incorporated radioactivity was detected by exposure of the gel to an X-ray film for 16h at -80°C (B).

The goal of the first experiment was to verify that CD25 is a target for ADP-ribosylation on Yac-1 lymphoma cells. For this purpose, the cells were harvested, washed and incubated with radiolabeled [³²P]-NAD⁺ (2,5 µCi, 0,4 µM) for 20 minutes at 37°C. Cells were lysed in PBS containing 1% Triton-X100 for 20 min at 4°C, and the cell lysate was cleared by centrifugation. In order to specifically isolate CD25 from the cell lysate, the lysate was immunoprecipitated with an anti-CD25 antibody (PC61) coupled to sepharose beads. As a control, a mock immunoprecipitation with protein-G coupled to sepharose beads was performed. The cell lysates were incubated with the matrix for 60 minutes at 4°C. Beads were washed (PBS, 1% Triton-X 100) and bound proteins were eluted from the matrix by incubation in SDS-PAGE sample buffer for 10 minutes at 70°C and separated from the matrix by centrifugation at 13000 rpm for 1 minute. The protein was contained in the supernatant. Soluble proteins in total cell lysates and the immunoprecipitates were size fractionated on precast SDS-PAGE gels. Proteins were detected by Coomassie staining of the gels. For detection of radiolabeled proteins, the gel was exposed to an X-ray film at -80°C for 18 – 72 hours.

The results show that multiple bands are radiolabeled, including a prominent broad band of 55kD (Figure 5.1B, lane 1), which was precipitated by immobilized anti-CD25 (lane 4). Consistently, immunoprecipitation with CD25-specific antibodies depleted this band from Yac-1 cell lysates (Figure 5.1B, lane 2). The control immunoprecipitation in lane 3 shows that no other ADP-ribosylated target proteins bound unspecifically to the sepharose beads used for immunoprecipitation.

Thus, CD25, the α chain of the IL-2R, is one major target of the ADP-ribosyltransferase ART2.2 on Yac-1 lymphoma cells. In the following sections, the repercussions of ADP-ribosylation of CD25 on the biological function of the IL-2R are assessed on the following levels: IL-2 binding, STAT5 phosphorylation and cell proliferation.

5.2 ADP-ribosylation blocks IL-2 binding and signaling

The heterotrimeric high-affinity receptor, expressed mainly on regulatory T cells and activated T effector cells, consists of CD25, CD122 and CD132. IL-2 binding results in the initiation of various signal transduction pathways, namely the MAP kinase pathway, the PI3 kinase pathway and the JAK STAT pathway. IL-2 acts as a growth factor and is important for the maintenance of regulatory T cells (Malek, 2008, Fontenot et al., 2005).

In order to assess whether ADP-ribosylation of CD25 affects the binding of IL-2, CTLL-2 cells, a murine cytotoxic T cell line, were used. These cells are IL-2 dependent, i.e. they cannot produce IL-2, and stop dividing in the absence of IL-2. CTLL-2 cells express CD25 at high levels but in contrast to Yac-1 cells, CTLL-2 cells show little if any endogenous ART2.2 expression or ART activity. Therefore, experiments were performed with untransfected CTLL-2 cells as well as with CTLL-2 cells stably transfected with ART2.2 (Figure 5.2).

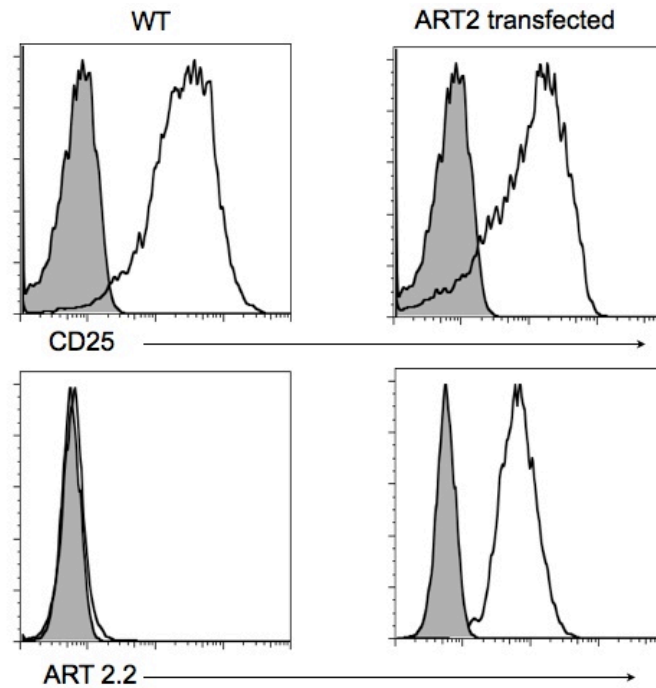


Figure 5.2: CD25 and ART2.2 expression on untransfected CTLL-2 cells (left) and CTLL-2 cells stably transfected with ART2.2 (right). The suspension cells were incubated with APC conjugated anti CD25 (PC61, 0,2 $\mu\text{g/ml}$) and FITC-conjugated anti ART2.2 (NikaA9, 0,2 $\mu\text{g/ml}$) for 15 minutes at 4°C. Cells were then washed and bound antibodies were detected by flow cytometry (open histograms). Unstained cells served as negative controls (grey shaded histograms).

A FACS-based IL-2 binding assay was performed with CTLL-2 cells using biotinylated IL-2 (R&D Systems) and fluorochrome-conjugated streptavidin. In order to determine the optimal detection sensitivity and the optimal IL-2 and streptavidin concentrations, an assay was performed with two different concentrations of streptavidin and biotinylated IL-2 (Figure 5.3).

The results show that FITC-conjugated streptavidin yielded weaker signals than the PE- and APC-conjugates (Figure 5.3A). PE- and APC-conjugated streptavidin resulted in stronger, dose-dependent signals with best resolution at the higher concentration combinations (Figure 5.3 B and C). For subsequent analyses, we chose a combination of 30 ng biotinylated IL-2 and 200 ng APC-conjugated streptavidin (corresponding to molar ratio of approximately 1:1).

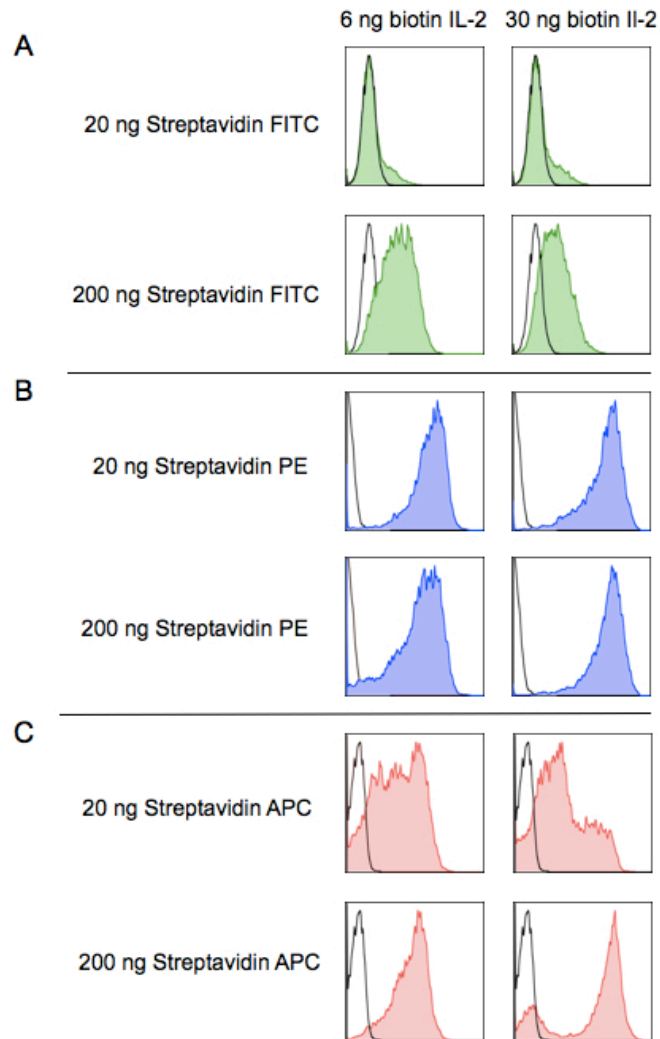


Figure 5.3: Biotinylated IL-2 detected on CTLL-2 cells with streptavidin conjugated to the fluorochromes FITC (green), PE (blue) and APC (red). 2×10^5 cells were incubated with two different amounts of biotinylated human IL-2 (6 ng, 30 ng) or with biotinylated soybean trypsin inhibitor (STI) (10 ng) as a negative control (black lines) for 30 minutes at 4°C (in 60 μ l PBS+/, 0,1% BSA). Immediately afterwards, i.e. without washing of the cells, the streptavidin conjugates were added (20 ng or 200 ng in 1 or 10 μ l PBS) and the cell suspensions were incubated for another 30 minutes at 4°C. The cells were washed twice and bound streptavidin was detected by flow cytometry.

In order to assess whether ADP-ribosylation of cell surface proteins affects the binding on IL-2, untransfected and ART2.2-transfected CTLL-2 cells were preincubated for 15 min in the absence or presence of NAD⁺ at 4°C. Cells were then incubated with biotinylated IL-2 for 60 minutes at 4°C and with APC-conjugated streptavidin for 30 minutes at 4°C. As a control, a parallel aliquot of cells was preincubated with an excess of unlabeled IL-2.

The results presented in Figure 5.4A show clear staining of both untransfected (WT) and ART2.2-transfected cells with APC-conjugated streptavidin after incubation with biotinylated IL-2 (red histograms) but little if any staining after control-incubations with biotinylated soybean trypsin inhibitor (STI, black histogram). Consistently, preincubation with unlabeled IL-2 completely blocked binding of biotinylated IL-2 to

both untransfected CTLL-2 cells as well as ART2.2 transfected CTLL-2 cells (Figure 5.4A). In contrast, preincubation with NAD^+ inhibited binding of IL-2 to ART2.2 transfected cells but not to untransfected cells (Figure 5.4B, blue histograms). Thus, NAD^+ -dependent ADP-ribosylation of cell surface proteins inhibits IL-2 binding.

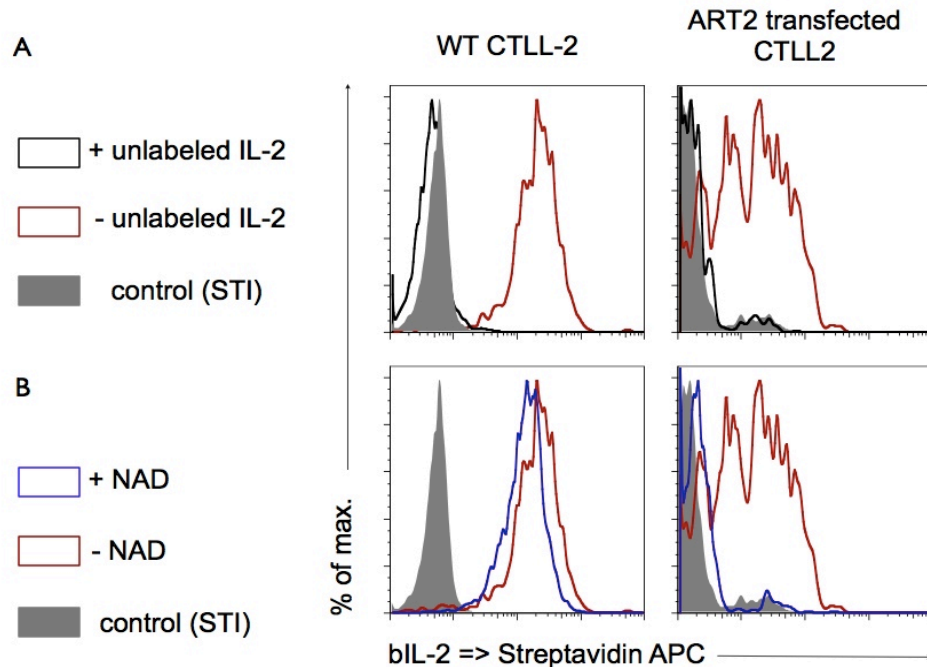


Figure 5.4: Extracellular NAD^+ inhibits IL-2 binding to ART2.2-transfected CTLL-2 cells. Untransfected and ART2.2-transfected CTLL-2 cells (10^5 cells) were preincubated in the absence or presence of unlabeled mouse IL-2 (500 ng) or NAD^+ (25 μM) for 15 min at 4°C in 30 μl PBS. Without a washing step, biotinylated human IL-2 (30 ng) or biotinylated soybean trypsin inhibitor (STI) (50 ng) was added and cells were incubated for 60 min at 4°C . Subsequently, again without washing, APC-conjugated Streptavidin (200 ng) was added and cells were incubated for 30 min at 4°C . Cells were then washed twice and analyzed by flow cytometry.

Upon binding of IL-2, one of the initiated signal transduction pathways is the JAK-STAT pathway, in which STAT5 is activated by phosphorylation. In order to determine whether ADP-ribosylation affects IL-2 induced STAT-5 signaling of primary mouse T cells, cells were prepared from the spleens of two ART2^{-/-} and two wildtype mice on the C57BL/6 DREG background. After lysis of erythrocytes, B cells were depleted using magnetic beads coated with anti-IgG (Dynabeads M-280 sheep anti-rabbit IgG).

1×10^6 cells were incubated in RPMI medium with or without 13 μM NAD^+ for 5 minutes at 37°C in a water bath. Cells were then stained with a V450 conjugated anti-CD4 monoclonal antibody for 30 minutes at 4°C (1:100) and, after two washing steps, further incubated in RPMI medium with or without 25 U/ml IL-2 (2,5 ng/ml) for 15 minutes at 37°C . Cells were fixed with 2% PFA for 10 minutes at 37°C and 90% methanol for 1 hour at 4°C . Cells were stained with anti-phospho STAT5 antibody and analyzed in the flow cytometer (Figure 5.5).

The results show that the majority of Tregs (GFP⁺ CD4⁺ T cells) as well as a small subset of GFP-negative CD4⁺ T cells respond to IL-2 by phosphorylating STAT5 in case of both, wildtype (panel 3) and ART2^{-/-} cells (panel 4). In the case of wildtype cells, pretreatment with NAD⁺ inhibited STAT5 phosphorylation in approximately 50% of the Treg population and 75% of the subset of GFP-negative CD4 T cells (panel 5) (Figure 5.5B). The inhibitory effect of NAD⁺ on STAT-5 phosphorylation was not observed in cells from ART2^{-/-} mice, indicating that the effect requires ART2.2-catalyzed ADP-ribosylation of cell surface proteins (Figure 5.5A, panel 6).

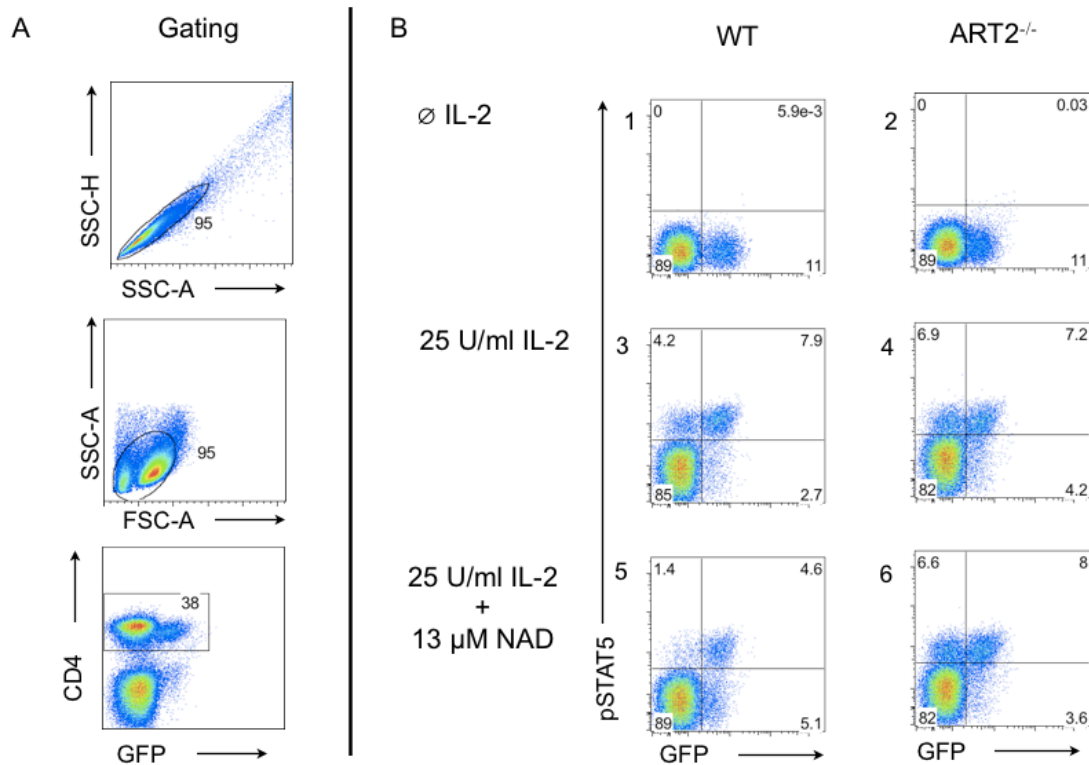


Figure 5.5: NAD⁺ inhibits STAT5 phosphorylation in CD4 positive cells. Spleen cells obtained from ART2^{-/-} or wildtype C57BL/6 mice carrying the DEREK transgene were depleted of B cells using magnetic beads coated with anti-mouse IgG antibodies at 4°C. Cells were preincubated in the absence or presence of 13 µM NAD⁺ for 5 minutes at 37°C. Cells were stained with V450-conjugated anti-CD4 for 30 min at 4°C and washed twice. Cells were resuspended in RPMI medium containing recombinant mouse IL-2 (10⁶ cells, 0.5ng IL-2/200 µl) (25U IL-2/ml) and incubated for 15 min at 37°C. Cells were then fixed in 2% paraformaldehyde (15 min at 37°C) and 90% methanol (1h 4°C) before staining with an APC-conjugated anti-phospho-STAT5 antibody A). Gating strategy: doublets were excluded in SSC-H vs. SSC-A and gating was performed on CD4⁺ cells. B) GFP in these mice is expressed from the DEREK transgene under control of the Foxp3 promoter. Regulatory T cells, therefore, appear as GFP⁺ cells.

In order to specifically examine the Treg population and to eliminate any effects mediated by ADP-ribosylation of P2X7 (Adriouch et al., 2008), a second experiment examining the effects of NAD⁺ on IL-2-induced phosphorylation of STAT-5 was performed with purified Tregs from ART2^{-/-} and P2X7^{-/-} mice. For this purpose, cells were prepared from the spleens of two ART2^{-/-} and two P2X7^{-/-} mice on the C57BL/6 background. After lysis of erythrocytes and depletion of B cells by anti-IgG Dynabeads a second magnetic sorting step was performed. To this end, cells were labeled with

unconjugated rat anti-mouse CD8a and CD11b antibodies for 20 minutes at 4°C. The cell suspension was depleted of antibody-covered cells with Dynabeads (M-450) coated with sheep anti-rat IgG. The CD25⁺ Treg population was then separated from the CD25⁻ population by positive magnetic cell sorting. For this purpose, the cell suspension was incubated with PE-conjugated anti-CD25 antibody (FD4) for 15 minutes at 4°C. Anti-PE-antibody coated MicroBeads (Miltenyi) were added and the cell suspension was transferred to a column placed in a strong magnetic field. The flowthrough containing the CD25⁻ T_H cell population was collected and the CD25⁺ population was washed off the column. Cells were counter-stained with a V450-conjugated anti-CD4 antibody. Aliquots of unsorted and sorted cells were analyzed by flow cytometry (Figure 5.6).

The results show that after depletion of B cells, CD8⁺ T cells and CD11b⁺ APCs, approximately 80% of the remaining cells were CD4⁺ (70% CD25⁻ and 10% CD25⁺) (panels 2 and 4). After separation of CD25⁺ cells, the purity of the CD4⁺/CD25⁻ naive Th cells was approximately 80% (panels 6 and 8), while the CD4⁺CD25⁺ Treg cell purity exceeded 90% (panels 10 and 12).

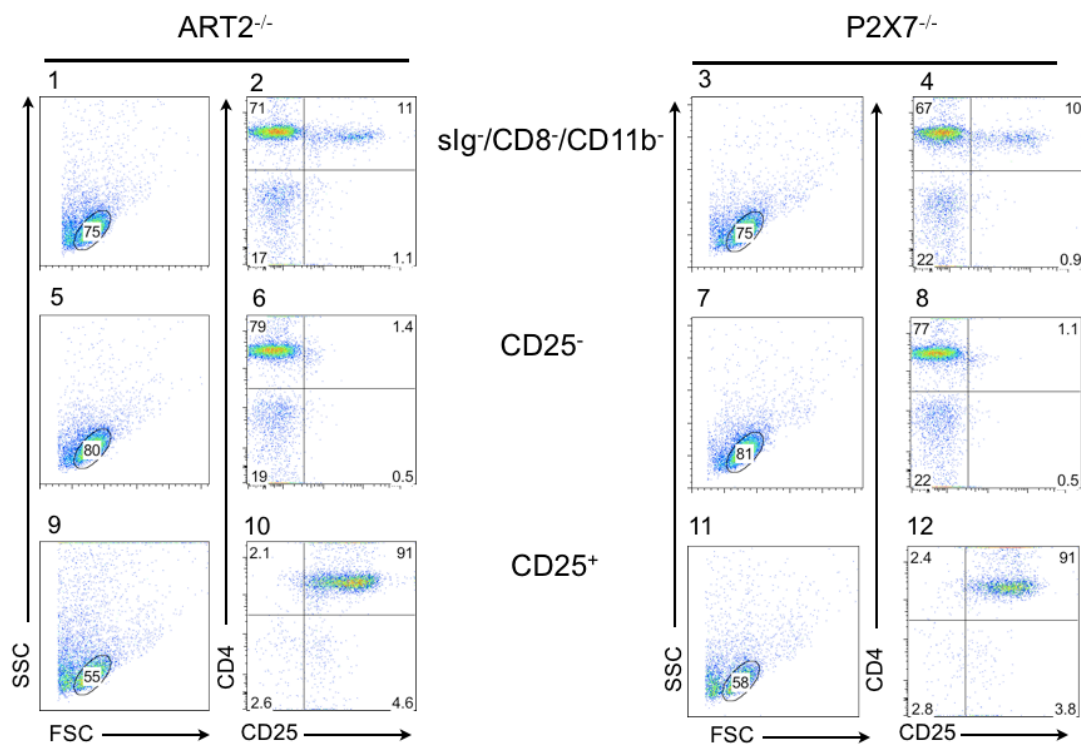


Figure 5.6: Purity of isolated regulatory T cells after magnetic cell sorting. Spleen cells obtained from ART2^{-/-} and P2X7^{-/-} mice (C57BL/6 background) were depleted of B cells using anti mouse IgG-coated Dynabeads (Invitrogen). CD8⁺ cells were coated with an anti-CD8a antibody and monocytes and macrophages with an anti-CD11b antibody, which were then depleted with anti rat IgG Dynabeads. After staining with PE-conjugated anti-CD25 (7D4), the CD25⁺ Treg population was isolated by positive magnetic cell sorting using anti-PE conjugated magnetic beads (miltenyi). Cells were counterstained with V450-conjugated anti-CD4 and purity of the cells was monitored by analyzing an aliquot of cells by flow cytometry.

The purified Tregs were preincubated with or without 100 μM NAD^+ for 10 minutes at 4°C. IL-2 was added for 15 minutes at 37°C. Cells were then fixed with 2% PFA and 90% methanol. The cells were then stained with an anti-phospho-STAT5 antibody and analyzed by flow cytometry (Figure 5.7).

The results show that, upon addition of IL-2, the majority of Tregs react with STAT5 phosphorylation (Figure 5.7). Preincubation with NAD^+ inhibited STAT5 phosphorylation in approximately 50% of the $\text{P2X7}^{-/-}$ cells (B). NAD^+ , however, did not show any inhibitory effect on STAT-5 phosphorylation by $\text{ART2}^{-/-}$ cells, indicating that the effects of NAD^+ on STAT5 depend on ART2.2-catalyzed ADP-ribosylation of cell surface proteins (A).

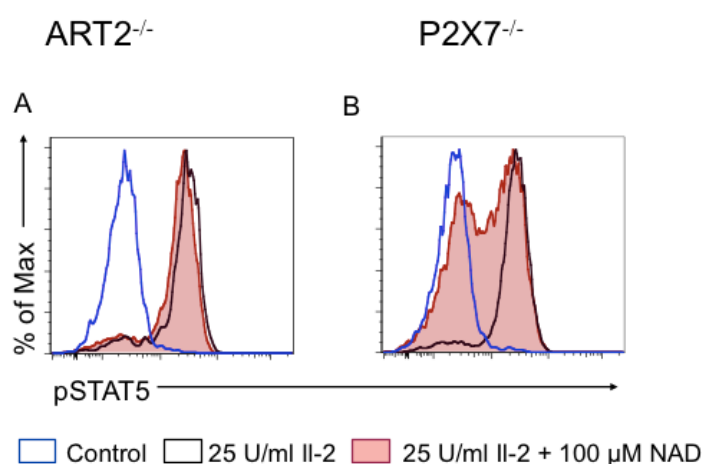


Figure 5.7: Extracellular NAD^+ inhibits IL-2 induced phosphorylation of STAT5 in regulatory T cells. Tregs isolated from $\text{ART2}^{-/-}$ or $\text{P2X7}^{-/-}$ mice were incubated in the absence (blue) or presence (black) of IL-2 for 15 minutes at 37°C. A parallel aliquot of cells was pre-incubated with 100 μM NAD^+ for 10 minutes at 4°C before the addition of IL-2 (red). After fixation of the cells, STAT5 phosphorylation was detected with an APC-conjugated anti-phospho-STAT5 antibody.

5.3 ADP-ribosylation blocks IL-2 dependent proliferation

In order to assess whether ADP-ribosylation of CD25 affects the downstream effects of IL-2 binding, the proliferation of untransfected and ART2.2-transfected CTLL-2 cells was assessed with and without the addition of NAD^+ .

Cells were depleted of IL-2 by washing in PBS twice followed by a 6 h incubation in complete medium lacking IL-2. Cells were then seeded in 24-well plates in medium containing serial dilutions of IL-2. Medium containing or lacking NAD^+ was added every 12 hours and cells were cultivated for 5 days before cell numbers were assessed by flow cytometry using Tru Count beads.

The results confirm that proliferation of CTLL-2 cells is IL-2 dependent (Figure 5.8). At low levels of IL-2, NAD^+ inhibits proliferation of cells expressing ART2.2 but not of untransfected cells. This indicates that the inhibitory effect of NAD^+ on cell proliferation is mediated by ART2.2-catalyzed ADP-ribosylation of cell surface proteins. These results are consistent with the previous findings that ADP-ribosylation

of cell surface proteins interferes with IL-2 binding (Figure 5.4) and phosphorylation of STAT5 (Figure 5.5). Note that the inhibitory effect of NAD^+ on cell proliferation of ART2^+ was most pronounced at low concentrations of IL-2 (0,2-5 ng/ml).

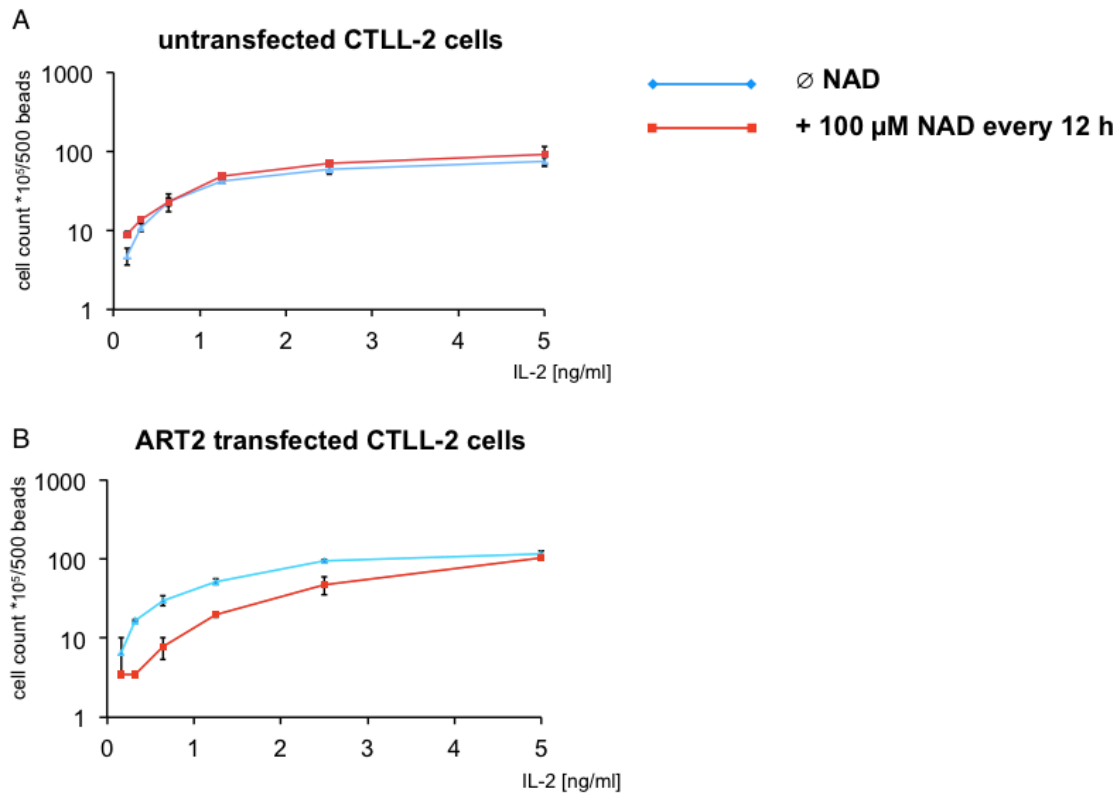


Figure 5.8: Extracellular NAD^+ inhibits the IL-2-dependent proliferation of ART2.2-transfected CTLL-2 lymphoma cells. Triplets of untransfected CTLL-2 cells (A) and CTLL-2 cells stably transfected with ART2.2 (B) were seeded in a 24 well culture plate (3×10^4 /well) and incubated for 3.5 days in 1 ml complete medium containing serial dilutions of human recombinant IL-2 (5 ng/ml, 2.5 ng/ml, 1.25 ng/ml, 0.64 ng/ml, 0.32 ng/ml and 0.16 ng/ml) (2.5-0.08 U/ml). Medium (10 μ l) lacking (blue) or containing NAD^+ (final concentration 100 μ M) (red) was added every 12 hours. Cells were harvested, stained with propidium iodide, and numbers of living (PI-negative) cells were quantified by flow cytometry with the aid of true-count beads.

5.4 CD25 is ADP-ribosylated on arginine residues 35, 36 and 117

The extracellular domain of CD25 contains eleven arginine residues, eight of which are resolved in the 3D structure of human CD25 (Fig. 5.9). Figure 5.9 illustrates their localization within the 3D structure (A) and the amino acid sequence (B) of the protein. Two of these arginine residues (R35, R36) lie within the IL-2 binding domain. (Robb et al., 1988, Stauber et al., 2006).

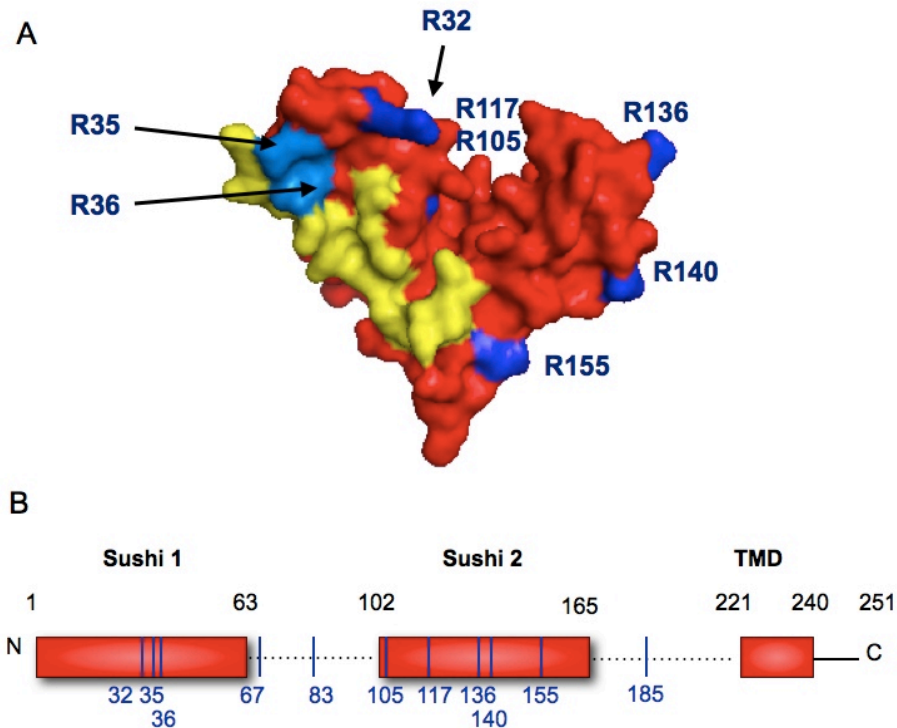


Figure 5.9: Schematic diagrams of the arginine residues in the extracellular domain of human CD25. A) 3D surface model of CD25 with the IL-2 binding site highlighted in yellow and the 8 arginines visible in the crystal structure highlighted in blue. B) Schematic diagram of the 11 arginine residues in the extracellular domain of hCD25. The blue numbers correspond to the position within the amino acid sequence of the native protein (i.e. after cleavage of the signal peptide). CD25 is composed of two Sushi domains, which encompass residues 22-84 and 123-186. The dotted lines indicate sections of CD25 that are unordered and not visible in the crystal structure. TMD: transmembrane domain. The 3D model was generated with pymol using the coordinates of CD25 in the co-crystal of human IL-2, CD25, CD122, and CD132 (pdb code 2erj).

In order to verify that ART2.2 ADP-ribosylates CD25 on arginine residues, we purchased a synthetic cDNA construct, in which all 11 arginines of human CD25 (hCD25) were substituted by lysine (R all K) and cloned it into the pCMVSPORT6 vector.

Plasmids encoding the RallK mutant or the wildtype hCD25 were cotransfected into HEK-T cells together with an expression construct for ART2.2. Cell surface expression levels were assessed 20 hours post transfection by flow cytometry, using a monoclonal anti-CD25 antibody (Figure 5.10A). The results confirm that the RallK mutant is expressed on the cell surface at levels superceding those of WT CD25. 48 hours post-transfection, cells were incubated with radioactively labeled $^{32}\text{P-NAD}^+$. Proteins were size fractionated by SDS-PAGE and then analyzed for the presence of CD25 by immunoblotting with a CD25-specific antibody and for covalently (SDS-resistant) incorporated radioactivity by autoradiography. The results show a radiolabeled band of 55 kD in cells transfected with CD25, whereas no radiolabeled bands were detectable in untransfected cells or in cells transfected with RallK, the mutant in which all arginines were mutated to lysine (Figure 5.10B). Western-Blot analyses show a stronger band in cells transfected with RallK than in cells transfected with WT CD25. Note that this band migrates with a slightly lower apparent molecular weight than WT CD25. The results

show that substitution of all arginine residues in the extracellular domain of CD25 by lysine precludes ADP-ribosylation by ART2.2, consistent with the notion that ADP-ribosylation of CD25 by ART2.2 is arginine-specific.

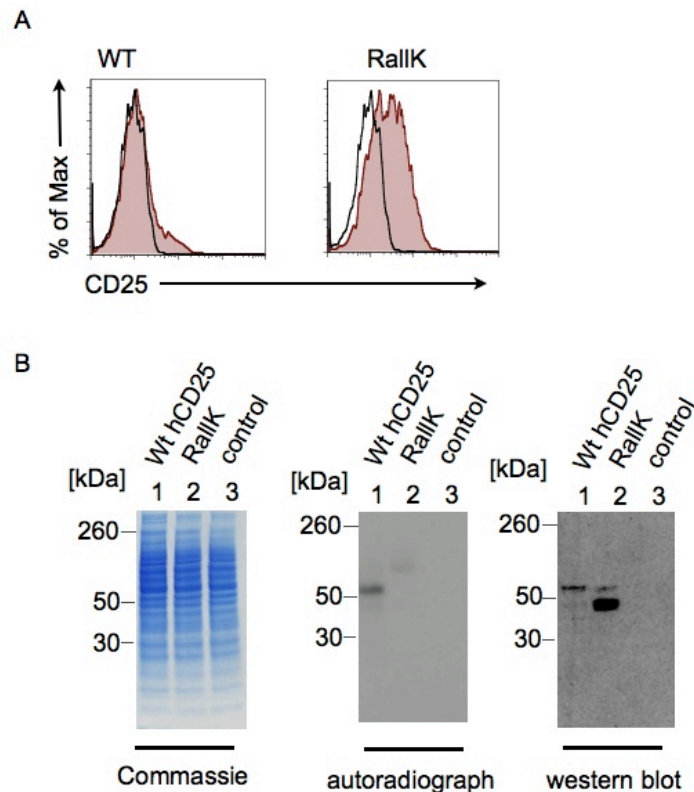


Figure 5.10: ADP-ribosylation of CD25 is arginine-dependent. HEK-T cells were cotransfected with expression vectors for ART2.2 and either wild type human CD25 or the complete mutant RallK. Control cells were transfected with a vector encoding GFP. Cells were harvested 20 h post transfection and stained with APC-conjugated anti-CD25 antibody (M-A251) before FACS analyses (red histograms, A). Cells were gated on living cells. 48 hours post transfection, the cells were incubated with [32 P]-NAD $^{+}$ for 20 minutes at 37°C, and then lysed in 1% Triton-X100. Lysates were cleared by centrifugation and soluble proteins were separated by gel electrophoresis (B). Total protein was visualized by Coomassie staining. Radiolabeled proteins were detected by exposing the gel to an X-ray film for 6 days at -80°C (B). In addition, CD25 was detected by western blotting with a polyclonal rabbit anti CD25 antibody.

In order to identify the specific target arginines, selected arginines in CD25 were mutated to lysine by site-directed mutagenesis. Each mutation was verified by DNA sequence analysis. Each hCD25 mutant was cotransfected into HEK-T cells with ART2.2 and analyzed for radioactive labeling upon incubation with 32 P-NAD $^{+}$. In a previous study, each of the single arginine to lysine mutants had been shown to be radiolabeled by ART2.2, indicating modification at more than one site (Hann, 2008). This is reminiscent of previous reports on the ADP-ribosylation of P2X7, LFA1 and defensin 1, all of which are ADP-ribosylated at more than one arginine (Laing et al., 2010, Paone et al., 2006, Adriouch et al., 2008, Laing et al., Nemoto et al., 1996).

Considering that the primary ADP-ribosylation sites on P2X7 and defensin 1 are double arginines and that the single mutants R35K, R36K and R117K showed lower radiolabeling than other mutants (Hann, 2008), a triple mutant was generated. Again,

this mutant and wildtype CD25 were cotransfected with ART2.2 into HEK-T cells. Control cells were cotransfected with P2X7 and ART2.2. Cell surface expression levels of CD25 were analyzed by FACS 48 hours after transfection. The results show slightly higher cell surface expression of the triple mutant than of WT CD25 (Figure 5.11A). Incorporation of radioactivity was analyzed as before after incubation of cells with [³²P]-NAD⁺. The results show much weaker radiolabeling of the triple mutant than of wildtype CD25, despite the higher cell surface expression level of the mutant. These results are consistent with the notion that CD25 is ADP-ribosylated mainly at these three sites (Figure 5.11).

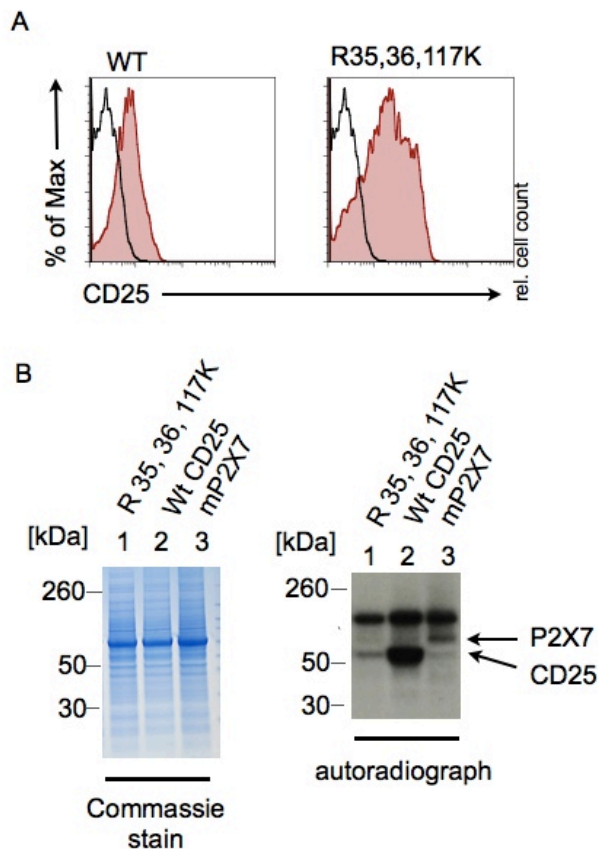


Figure 5.11: Identification of R35, R36, and R117 as the major ADP-ribosylation sites on CD25. HEK-T cells were cotransfected with expression vectors for ART2.2 and either wild type human CD25, the triple mutant R35, 36, 117K, or P2X7 for control. Cells were harvested 48 h post transfection and stained with APC-conjugated anti-CD25 antibody (M-A251) before FACS analyses (red histograms, A). 48 hours post transfection, the cells were incubated with [³²P]-NAD⁺ for 20 minutes at 37°C, and then lysed in 1% Triton-X100. Lysates were cleared by centrifugation and soluble proteins were separated by gel electrophoresis (B). Total protein was visualized by Coomassie staining. Radiolabeled proteins were detected by exposing the gel to an X-ray film for 6 days at -80°C (B).

6 Discussion

The results presented here identify CD25, the α chain of the IL-2 receptor, as a major target of ART2.2 (Figure 5.1) and provide insight into the role of ADP-ribosylation of CD25.

ADP-ribosylation assays with CD25 mutants confirm that CD25 is ADP-ribosylated on arginine residues (Figure 5.10) and indicate that residues R35, R36 and/or R117 are the main ADP-ribosylation sites (Figure 5.11). This is reminiscent of murine P2X7 and human defensin 1, both of which contain double arginines as primary sites of ADP-ribosylation, but are additionally ADP-ribosylated on other arginines residues (Adriouch et al., 2008, Paone et al., 2006). The fact that CD25 is ADP-ribosylated at more than one arginine residue makes it difficult to identify the target arginines only by site directed mutagenesis. Moreover, the accessibility of the target arginine to enzymatic modification may be influenced by structural or conformational changes of the target protein caused by amino acid replacement or posttranslational modification of other residues. Such an effect was reported for ras, the target for ADP-ribosylation by the *Pseudomonas* toxin exoS: mutation of the two major ADP-ribosylation sites in ras, R41 and R128 to lysine, resulted in the ADP-ribosylation of an alternative arginine (R135) (Ganesan et al., 1998, Ganesan et al., 1999b). This may also pertain to the ADP-ribosylation of CD25 by ART2.2, where residual incorporation of radioactivity is still observed in the triple mutant R35KR36KR117K (Figure 5.11). Conceivably, back mutation of single or multiple sites in the RallK mutant, would yield further insight into which arginine residues in CD25 - either individually or in combination - can serve as targets. Mass spectrometry presents a complementary approach for the identification of target sites (Laing et al., 2010, Ganesan et al., 1999b, Paone et al., 2006, Ganesan et al., 1999a). The extensive glycosylation of CD25 at N- and O- linked positions makes such analyses difficult (Malek, 2008). Further, it is conceivable that the binding of other proteins may induce conformational changes and/or sterically block access of the ART to potential target arginines (Zolkiewska, 2005). Similarly, the accessibility of target arginines in CD25 might be influenced by binding of IL-2 and/or the beta and gamma chains of the receptor.

The molecular basis for the specificity of ART2.2 for a certain target protein and a target residue remains yet to be fully clarified. ART2.2 carries the R-S-EXE motif common to all known arginine-specific ADP-ribosyltransferases (Koch-Nolte et al., 2008, Hottiger et al., 2010). ART2.2 can ADP-ribosylate a broad range of targets, and in this aspect resembles the exoS and exoT toxins from *Pseudomonas aeruginosa* (Sun et al., 2004) and ADP-ribosyltransferases of *E.coli* T-phages (Depping et al., 2005). The preference of the more specific bacterial ADP-ribosyltransferases such as SpvB (*Salmonella enterica* toxin) and C2 (*Clostridium botulinum* toxin) for a single arginine residue in a single target protein (Arg177 of actin) likely is largely controlled by structural complementarity of the toxin to its target, as revealed by co-crystallization of C2 toxin and actin (Tsuge et al., 2008). ART2.2 is one of the more promiscuous ADP-ribosyltransferases that have a variety of target proteins (Laing et al., 2010, Koch-Nolte

et al., 1996b). Here, structural complementarity seems to play a less stringent role. Other *in vivo* factors may be important, such as accessibility of the target proteins to the enzyme by, for example, cellular compartmentalization (Koch-Nolte et al., 2011). Thus, the ecto-enzyme ART2.2 only has access to surface-bound proteins, where accessibility is further regulated by lipid raft association (Bannas et al., 2005) and the proximity of the catalytic domain to the cell membrane (Zolkiewska, 2005).

It is conceivable that ADP-ribosylation of CD25 operates synergistically with ADP-ribosylation of other cell surface proteins such as P2X7 and LFA-1 (Scheuplein et al., 2009). As a downstream effect, the ADP-ribosylation of P2X7 induces shedding of CD62L and CD27, whereby reducing the capacity of the cells to migrate, and further induces the externalization of phosphatidylserine and cell death (Seman et al., 2003), (Hubert et al., 2010). On the other hand, the ADP-ribosylation of LFA-1, which is expressed ubiquitously on T cells, blocks the capacity of the cell to bind to ligands on other cells, whereby inactivating the protein's function (Nemoto et al., 1996). These functional consequences of ADP-ribosylation might, in association with the reduced capacity to proliferate, be three synergistic means of influence regulatory T cell function *in vivo*.

The arginine residues R35 and R36 are localized within the IL-2 binding site of CD25 (Figure 5.9A). As ADP-ribosylation attaches a bulky residue and converts a positively charged arginine into a negatively charged ADP-ribosylarginine, it is likely that ADP-ribosylation sterically interferes with IL-2 binding. Our results show that ADP-ribosylation of CD25, indeed, inhibits binding of IL-2 (Figure 5.4). This could explain the observed downstream effects following incubation of cells with NAD⁺, i.e. inhibition of STAT5 phosphorylation by Tregs (Figure 5.7) and the inhibition of IL-2 dependent proliferation of CTLL-2 cells (Figure 5.8).

Considering that ADP-ribosylation of CD25 inhibits binding of IL-2, it is tempting to speculate that this may provide a regulatory mechanism to divert IL-2 from CD25-dependent signaling to CD25-independent signaling by CD122/CD132, i.e. from Tregs to NK cells and to CD8⁺ cytotoxic T cells (Figure 6.1). In a non-inflammatory environment, where the concentration of extracellular NAD⁺ is low, consumption of extracellular IL-2 by Tregs would deprive other T cells and NK cells of IL-2 (Figure 6.1 B, C) (Pandiyani et al., 2007). Similarly, systemic injections of low doses of IL-2 may result in the preferential expansion of Tregs (Grinberg-Bleyer et al., 2011, Koreth et al., 2011, Saadoun et al., 2011). In an inflammatory environment with high concentrations of extracellular NAD⁺, ADP-ribosylation of CD25 would divert IL-2 signaling away from Tregs to NK cells and CD8⁺ cytotoxic cells (Figure 6.1 C,F). This mechanisms of tuning IL-2 signaling may be mimicked by certain IL-2 antibodies used *in vivo* (Figure 6.1D): systemic injection of mouse IL-2 complexed with S4B6 or JES6-5HA or of human IL-2 complexed with Mab-602 causes preferential expansion of NK cell and cytotoxic T cells (Boyman et al., 2006, Krieg et al., Krieg et al., 2010).

In addition to Tregs that constitutively express CD25, CD25 is also up-regulated by activated T cells following triggering of the T cell receptor (Figure 6.1F). Since T cell activation triggers metalloprotease-mediated shedding of ART2.2, activated T cells cannot ADP-ribosylate cell surface proteins (Kahl et al., 2000). However, it is unclear whether ART2.2 remains absent or low on the cell surface when activated T cells express CD25-if so, ADP-ribosylation of CD25 would be a Treg specific regulatory mechanism.

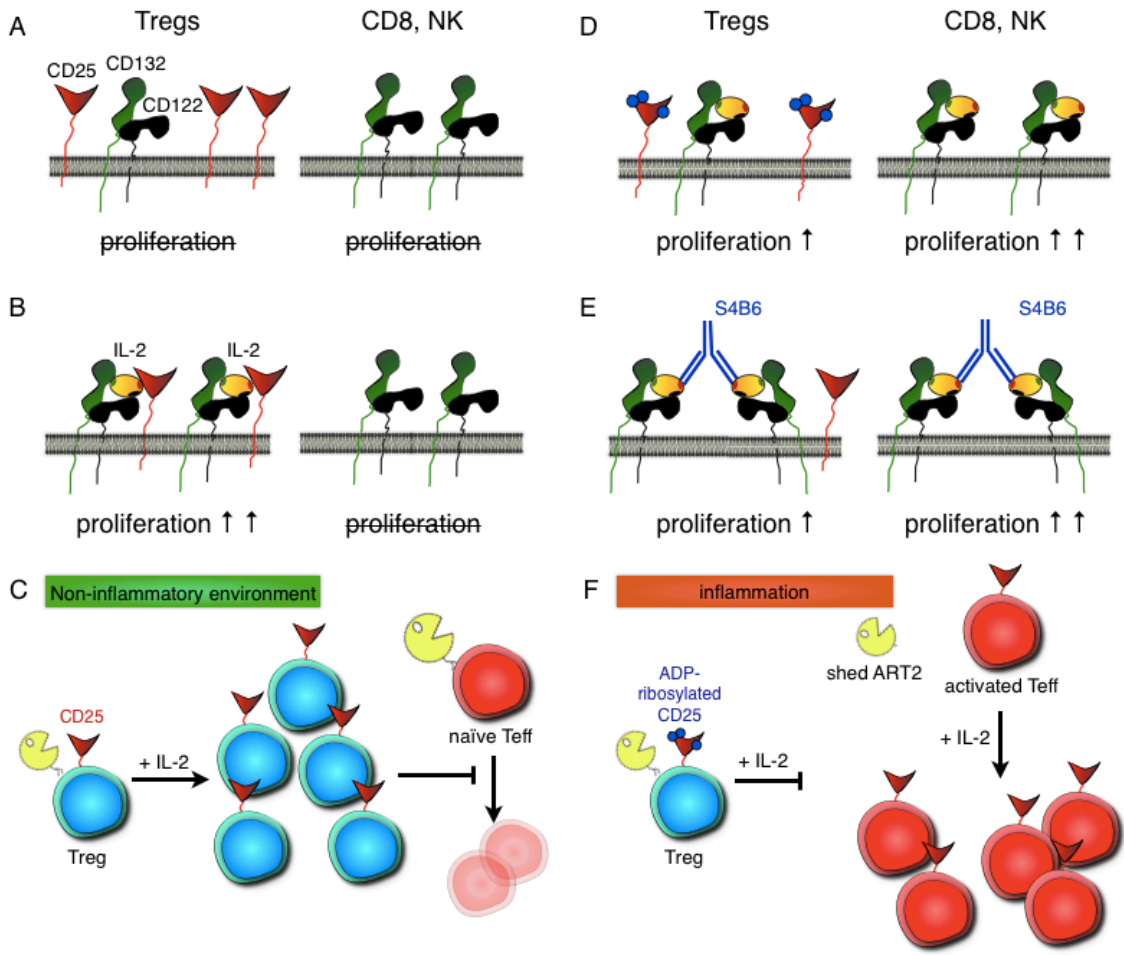


Figure 6.1: Model for the tuning of IL-2 signaling by ADP-ribosylation of CD25. A) Tregs constitutively express high levels of CD25 while CD8⁺ T cells and NK cells express only the β and γ chains of the IL-2R. B), C) In a non-inflammatory environment, IL-2 is consumed mainly by Tregs and cytokine-depletion prevents the proliferation of CD8⁺ cells and NK cells. D) In an inflammatory environment, i.e. following the release of NAD⁺ from damaged cells, ADP-ribosylation of CD25 diverts IL-2 from the high affinity receptor to the low affinity β and γ chains, resulting in the preferential expansion of CD8⁺ cells and NK cells. E) Systemic injection of IL-2 in complex with antibodies that prevent binding of IL-2 to CD25; similarly results in the preferential expansion of CD8⁺ cells and NK cells. F) In the presence of extracellular NAD⁺, ART2.2-catalyzed ADP-ribosylation of CD25 blocks the consumption of IL-2 by Tregs. Triggering of the T cell receptor on effector T cells (Teff) induces shedding of ART2.2 and up-regulation of CD25, thereby allowing efficient expansion of these cells.

In vivo, this mechanism for tuning signaling by IL-2 by ADP-ribosylation of CD25 likely depends on the context in which Tregs are exposed to NAD⁺. Thus, at sites where NAD⁺ is released in large quantities from damaged cells, such as during lytic viral infections, ADP-ribosylation of CD25 on Tregs would favor proliferation and function of CD8⁺ effector T cells, thereby enhancing pathogen eradication. In contrast, in healthy tissues, where little if any NAD⁺ is released, Treg function would not be inhibited by ADP-ribosylation, permitting efficient suppression of potentially autoreactive T effector cells.

7 Perspectives

The finding that CD25 is a target for ADP-ribosylation raises a number of questions that can be addressed in future studies. The remaining potential target arginines could be identified by further mutational analyses, for example a step-by-step remutagenesis of the RallK mutant into the wildtype. Potential effects of ADP-ribosylation on the proliferation of Tregs could be assessed by *in vitro* proliferation assays analogous to the ones performed with CTLL-2 cells, e.g. in the presence of a T cell receptor signal, appropriate co-stimulation and IL-2 (Shevach, 2009). The effects of ADP-ribosylation on Treg suppressor functions could be assessed in appropriate *in vitro* suppressor assays. Here, CFSE (Carboxyfluorescein succinimidyl ester) - labelled T effector cells and regulatory T cells are co-incubated in various ratios together with growth factors and, after 48 or 72 hours, T cell proliferation is measured by flow cytometry. We would expect a reduced inhibitory capacity of regulatory T cells subsequent to ADP-ribosylation of CD25 and other cell surface proteins, i.e. an increased proliferation of T effector cells.

8 Abbreviations

ADP	Adenosine diphosphate
ART	ADP-ribosyltransferasee
BAC	Bacterial artificial chromosoem
BSA	Bovine serum albumin
CFSE	Carboxyfluorescein succinimidyl ester
DEREG	Depletion of regulatory T cells
DTR	Diphtheria toxin receptor
EDTA	Ethylene diamine tetra acidic acid
FACS	Fluorescence activated cell sorting
Foxp3	Forkhead box protein 3
GFP	Green fluorescent protein
IL-2	Interleukin-2
IL-2R	Interleukin-2 receptor
IPEX	immune dysregulation, polyendocrinopathy, enteropathy, X-linked
mAb	Monoclonal antibody
NAD ⁺	Nicotinamide adenine dinucleotide
NICD	NAD ⁺ -induced cell death
STI	Soybean trypsin inhibitor
TGF- β	Transforming growth factor β
Th	T helper cells
Treg	Regulatory T cells
WT	Wildtype

9 Bibliography

- ABBAS, A. K., LICHTMAN, A. H. & PALLAI, S. 2007. Cellular and Molecular Immunology, Saunders Elsevier.
- ADRIOUCH, S., BANNAS, P., SCHWARZ, N., FLIEGERT, R., GUSE, A. H., SEMAN, M., HAAG, F. & KOCH-NOLTE, F. 2008. ADP-ribosylation at R125 gates the P2X7 ion channel by presenting a covalent ligand to its nucleotide binding site. *Faseb J*, 22, 861-9.
- AKTORIES, K. & BARBIERI, J. T. 2005. Bacterial cytotoxins: targeting eukaryotic switches. *Nat Rev Microbiol*, 3, 397-410.
- ALUVIHARE, V. R., KALLIKOURDIS, M. & BETZ, A. G. 2004. Regulatory T cells mediate maternal tolerance to the fetus. *Nat Immunol*, 5, 266-71.
- AOKI, C. A., ROIFMAN, C. M., LIAN, Z. X., BOWLUS, C. L., NORMAN, G. L., SHOENFELD, Y., MACKAY, I. R. & GERSHWIN, M. E. 2006. IL-2 receptor alpha deficiency and features of primary biliary cirrhosis. *J Autoimmun*, 27, 50-3.
- APOSTOLOU, I., SARUKHAN, A., KLEIN, L. & VON BOEHMER, H. 2002. Origin of regulatory T cells with known specificity for antigen. *Nat Immunol*, 3, 756-63.
- ASWAD, F., KAWAMURA, H. & DENNERT, G. 2005. High sensitivity of CD4+CD25+ regulatory T cells to extracellular metabolites nicotinamide adenine dinucleotide and ATP: a role for P2X7 receptors. *J Immunol*, 175, 3075-83.
- BANNAS, P., ADRIOUCH, S., KAHL, S., BRAASCH, F., HAAG, F. & KOCH-NOLTE, F. 2005. Activity and specificity of toxin-related mouse T cell ecto-ADP-ribosyltransferase ART2.2 depends on its association with lipid rafts. *Blood*, 105, 3663-70.
- BENSINGER, S. J., BANDEIRA, A., JORDAN, M. S., CATON, A. J. & LAUFER, T. M. 2001. Major histocompatibility complex class II-positive cortical epithelium mediates the selection of CD4(+)/25(+) immunoregulatory T cells. *J Exp Med*, 194, 427-38.
- BENSINGER, S. J., WALSH, P. T., ZHANG, J., CARROLL, M., PARSONS, R., RATHMELL, J. C., THOMPSON, C. B., BURCHILL, M. A., FARRAR, M. A. & TURKA, L. A. 2004. Distinct IL-2 receptor signaling pattern in CD4+CD25+ regulatory T cells. *J Immunol*, 172, 5287-96.
- BIELEKOVA, B., RICHERT, N., HOWARD, T., BLEVINS, G., MARKOVIC-PLESE, S., MCCARTIN, J., FRANK, J. A., WURFEL, J., OHAYON, J., WALDMANN, T. A., MCFARLAND, H. F. & MARTIN, R. 2004. Humanized anti-CD25 (daclizumab) inhibits disease activity in multiple sclerosis patients failing to respond to interferon beta. *Proc Natl Acad Sci U S A*, 101, 8705-8.
- BOYMAN, O., KOVAR, M., RUBINSTEIN, M. P., SURH, C. D. & SPRENT, J. 2006. Selective stimulation of T cell subsets with antibody-cytokine immune complexes. *Science*, 311, 1924-7.
- BRUNKOW, M. E., JEFFERY, E. W., HJERRILD, K. A., PAEPER, B., CLARK, L. B., YASAYKO, S. A., WILKINSON, J. E., GALAS, D., ZIEGLER, S. F. & RAMSDELL, F. 2001. Disruption of a new forkhead/winged-helix protein,

- scurfin, results in the fatal lymphoproliferative disorder of the scurfy mouse. *Nat Genet*, 27, 68-73.
- CAUDY, A. A., REDDY, S. T., CHATILA, T., ATKINSON, J. P. & VERBSKY, J. W. 2007. CD25 deficiency causes an immune dysregulation, polyendocrinopathy, enteropathy, X-linked-like syndrome, and defective IL-10 expression from CD4 lymphocytes. *J Allergy Clin Immunol*, 119, 482-7.
- CORDA, D. & DI GIROLAMO, M. 2003. Functional aspects of protein mono-ADP-ribosylation. *Embo J*, 22, 1953-8.
- CUROTTO DE LAFAILLE, M. A. & LAFAILLE, J. J. 2009. Natural and adaptive foxp3+ regulatory T cells: more of the same or a division of labor? *Immunity*, 30, 626-35.
- DAYER, J. M., FEIGE, U., EDWARDS, C. K., 3RD & BURGER, D. 2001. Anti-interleukin-1 therapy in rheumatic diseases. *Curr Opin Rheumatol*, 13, 170-6.
- DEPPING, R., LOHAUS, C., MEYER, H. E. & RUGER, W. 2005. The mono-ADP-ribosyltransferases Alt and ModB of bacteriophage T4: target proteins identified. *Biochem Biophys Res Commun*, 335, 1217-23.
- DI VIRGILIO, F., BOEYNAEMS, J. M. & ROBSON, S. C. 2009. Extracellular nucleotides as negative modulators of immunity. *Curr Opin Pharmacol*, 9, 507-13.
- DINARELLO, C. A. 2007. Historical insights into cytokines. *Eur J Immunol*, 37 Suppl 1, S34-45.
- FONTENOT, J. D., GAVIN, M. A. & RUDENSKY, A. Y. 2003. Foxp3 programs the development and function of CD4+CD25+ regulatory T cells. *Nat Immunol*, 4, 330-6.
- FONTENOT, J. D., RASMUSSEN, J. P., GAVIN, M. A. & RUDENSKY, A. Y. 2005. A function for interleukin 2 in Foxp3-expressing regulatory T cells. *Nat Immunol*, 6, 1142-51.
- FONTENOT, J. D. & RUDENSKY, A. Y. 2005. A well adapted regulatory contrivance: regulatory T cell development and the forkhead family transcription factor Foxp3. *Nat Immunol*, 6, 331-7.
- GANESAN, A. K., FRANK, D. W., MISRA, R. P., SCHMIDT, G. & BARBIERI, J. T. 1998. Pseudomonas aeruginosa exoenzyme S ADP-ribosylates Ras at multiple sites. *J Biol Chem*, 273, 7332-7.
- GANESAN, A. K., MENDE-MUELLER, L., SELZER, J. & BARBIERI, J. T. 1999a. Pseudomonas aeruginosa exoenzyme S, a double ADP-ribosyltransferase, resembles vertebrate mono-ADP-ribosyltransferases. *J Biol Chem*, 274, 9503-8.
- GANESAN, A. K., VINCENT, T. S., OLSON, J. C. & BARBIERI, J. T. 1999b. Pseudomonas aeruginosa exoenzyme S disrupts Ras-mediated signal transduction by inhibiting guanine nucleotide exchange factor-catalyzed nucleotide exchange. *J Biol Chem*, 274, 21823-9.
- GAVIN, M. A., TORGERSON, T. R., HOUSTON, E., DEROOS, P., HO, W. Y., STRAY-PEDERSEN, A., OCHELTREE, E. L., GREENBERG, P. D., OCHS, H. D. & RUDENSKY, A. Y. 2006. Single-cell analysis of normal and FOXP3-mutant human T cells: FOXP3 expression without regulatory T cell development. *Proc Natl Acad Sci U S A*, 103, 6659-64.

- GILLIS, S., BAKER, P. E., RUSCETTI, F. W. & SMITH, K. A. 1978. Long-term culture of human antigen-specific cytotoxic T-cell lines. *J Exp Med*, 148, 1093-8.
- GILLIS, S. & SMITH, K. A. 1977. Long term culture of tumour-specific cytotoxic T cells. *Nature*, 268, 154-6.
- GIRI, J. G., AHDIEH, M., EISENMAN, J., SHANEBECK, K., GRABSTEIN, K., KUMAKI, S., NAMEN, A., PARK, L. S., COSMAN, D. & ANDERSON, D. 1994. Utilization of the beta and gamma chains of the IL-2 receptor by the novel cytokine IL-15. *EMBO J*, 13, 2822-30.
- GLOWACKI, G., BRAREN, R., CETKOVIC-CVRLJE, M., LEITER, E. H., HAAG, F. & KOCH-NOLTE, F. 2001. Structure, chromosomal localization, and expression of the gene for mouse ecto-mono(ADP-ribosyl)transferase ART5. *Gene*, 275, 267-77.
- GLOWACKI, G., BRAREN, R., FIRNER, K., NISSEN, M., KUHL, M., RECHE, P., BAZAN, F., CETKOVIC-CVRLJE, M., LEITER, E., HAAG, F. & KOCH-NOLTE, F. 2002. The family of toxin-related ecto-ADP-ribosyltransferases in humans and the mouse. *Protein Sci*, 11, 1657-1670.
- GRINBERG-BLEYER, Y., BAEYENS, A., PIAGGIO, E. & SALOMON, B. L. 2011. [Could we cure type 1 diabetes by stimulating T(reg)?]. *Med Sci (Paris)*, 27, 471-2.
- HAAG, F., KOCH-NOLTE, F., KÜHL, M., LORENZEN, S. & THIELE, H. G. 1994. Premature stop codons inactivate the RT6 genes of the human and chimpanzee species. *J Mol Biol*, 243, 537-546.
- HANN, A. 2008. Die posttranslationale Modifikation des IL-2-Rezeptors durch ADP-Ribose. Med. Dissertation, Universität Medical Center Hamburg.
- HASSA, P. O. & HOTTIGER, M. O. 2008. The diverse biological roles of mammalian PARPs, a small but powerful family of poly-ADP-ribose polymerases. *Front Biosci*, 13, 3046-82.
- HONG, S., BRASS, A., SEMAN, M., HAAG, F., KOCH-NOLTE, F. & DUBYAK, G. R. 2007. Lipopolysaccharide, IFN-gamma, and IFN-beta induce expression of the thiol-sensitive ART2.1 Ecto-ADP-ribosyltransferase in murine macrophages. *J Immunol*, 179, 6215-27.
- HONG, S., BRASS, A., SEMAN, M., HAAG, F., KOCH-NOLTE, F. & DUBYAK, G. R. 2009. Basal and inducible expression of the thiol-sensitive ART2.1 ecto-ADP-ribosyltransferase in myeloid and lymphoid leukocytes. *Purinergic Signal*, 5, 369-83.
- HONJO, T., NISHIZUKA, Y., HAYAISHI, O. & KATO, I. 1968. Diphtheria toxin-dependent adenosine diphosphate ribosylation of aminoacyl transferase II and inhibition of protein synthesis. *J. Biol. Chem.*, 243, 3553-3555.
- HORI, S., NOMURA, T. & SAKAGUCHI, S. 2003. Control of regulatory T cell development by the transcription factor Foxp3. *Science*, 299, 1057-61.
- HORI, T., UCHIYAMA, T., TSUDO, M., UMADOME, H., OHNO, H., FUKUHARA, S., KITA, K. & UCHINO, H. 1987. Establishment of an interleukin 2-dependent human T cell line from a patient with T cell chronic lymphocytic leukemia who is not infected with human T cell leukemia/lymphoma virus. *Blood*, 70, 1069-72.

- HOTTIGER, M. O., HASSA, P. O., LUSCHER, B., SCHULER, H. & KOCH-NOLTE, F. 2010. Toward a unified nomenclature for mammalian ADP-ribosyltransferases. *Trends Biochem Sci*, 35, 208-19.
- HUBERT, S., RISSIEK, B., KLAGES, K., HUEHN, J., SPARWASSER, T., HAAG, F., KOCH-NOLTE, F., BOYER, O., SEMAN, M. & ADRIOUCH, S. 2010. Extracellular NAD⁺ shapes the Foxp3⁺ regulatory T cell compartment through the ART2-P2X7 pathway. *J Exp Med*, 207, 2561-8.
- JORDAN, M. S., BOESTEANU, A., REED, A. J., PETRONE, A. L., HOLENBECK, A. E., LERMAN, M. A., NAJI, A. & CATON, A. J. 2001. Thymic selection of CD4⁺CD25⁺ regulatory T cells induced by an agonist self-peptide. *Nat Immunol*, 2, 301-6.
- KAHL, S., NISSEN, M., GIRISCH, R., DUFFY, T., LEITER, E. H., HAAG, F. & KOCH-NOLTE, F. 2000. Metalloprotease-mediated shedding of enzymatically active mouse ecto-ADP-ribosyltransferase ART2.2 upon T cell activation. *J Immunol*, 165, 4463-9.
- KAMIMURA, D. & BEVAN, M. J. 2007. Naive CD8⁺ T cells differentiate into protective memory-like cells after IL-2 anti IL-2 complex treatment in vivo. *J Exp Med*, 204, 1803-12.
- KANAITSUKA, T., BORTELL, R., STEVENS, L. A., MOSS, J., SARDINHA, D., RAJAN, T. V., ZIPRIS, D., MORDES, J. P., GREINER, D. L. & ROSSINI, A. A. 1997. Expression in BALB/c and C57BL/6 mice of Rt6-1 and Rt6-2 ADP-ribosyltransferases that differ in enzymatic activity: C57BL/6 Rt6-1 is a natural transferase knockout. *J Immunol.*, 159, 2741-9.
- KIESSLING, R., KLEIN, E., PROSS, H. & WIGZELL, H. 1975. "Natural" killer cells in the mouse. II. Cytotoxic cells with specificity for mouse Moloney leukemia cells. Characteristics of the killer cell. *Eur J Immunol*, 5, 117-21.
- KOCH-NOLTE, F., ADRIOUCH, S., BANNAS, P., KREBS, C., SCHEUPLEIN, F., SEMAN, M. & HAAG, F. 2006. ADP-ribosylation of membrane proteins: unveiling the secrets of a crucial regulatory mechanism in mammalian cells. *Ann Med*, 38, 188-99.
- KOCH-NOLTE, F., DUFFY, T., NISSEN, M., KAHL, S., KILLEEN, N., ABLAMUNITS, V., HAAG, F. & LEITER, E. H. 1999. A new monoclonal antibody detects a developmentally regulated mouse ecto-ADP-ribosyltransferase on T cells: subset distribution, inbred strain variation, and modulation upon T cell activation. *J Immunol*, 163, 6014-22.
- KOCH-NOLTE, F., FISCHER, S., HAAG, F. & ZIEGLER, M. 2011. Compartmentation of NAD⁺-dependent signalling. *FEBS Lett*, 585, 1651-6.
- KOCH-NOLTE, F. & HAAG, F. 1997. Mono(ADP-ribosyl)transferases and related enzymes in animal tissues. Emerging gene families. *Adv. Exp. Med. Biol.*, 419, 1-13.
- KOCH-NOLTE, F., HAAG, F., KASTELEIN, R. & BAZAN, F. 1996a. Uncovered: the family relationship of a T-cell-membrane protein and bacterial toxins. *Immunol. Today*, 17, 402-5.
- KOCH-NOLTE, F., KERNSTOCK, S., MUELLER-DIECKMANN, C., WEISS, M. S. & HAAG, F. 2008. Mammalian ADP-ribosyltransferases and ADP-ribosylhydrolases. *Front Biosci*, 13, 6716-29.

- KOCH-NOLTE, F., KLEIN, J., HOLLMANN, C., KÜHL, M., HAAG, F., GASKINS, H. R., LEITER, E. H. & THIELE, H. G. 1995. Defects in the structure and expression of the genes for the T cell marker Rt6 in NZW and (NZB x NZW)F1 mice. *Internat. Immunol.*, 7, 883-890.
- KOCH-NOLTE, F., PETERSEN, D., BALASUBRAMANIAN, S., HAAG, F., KAHLKE, D., WILLER, T., KASTELEIN, R., BAZAN, F. & THIELE, H. G. 1996b. Mouse T cell membrane proteins Rt6-1 and Rt6-2 are arginine/protein mono(ADPribose)yltransferases and share secondary structure motifs with ADP-ribosylating bacterial toxins. *J. Biol. Chem.*, 271, 7686-93.
- KORETH, J., MATSUOKA, K., KIM, H. T., MCDONOUGH, S. M., BINDRA, B., ALYEA, E. P., 3RD, ARMAND, P., CUTLER, C., HO, V. T., TREISTER, N. S., BIENFANG, D. C., PRASAD, S., TZACHANIS, D., JOYCE, R. M., AVIGAN, D. E., ANTIN, J. H., RITZ, J. & SOIFFER, R. J. 2011. Interleukin-2 and regulatory T cells in graft-versus-host disease. *N Engl J Med*, 365, 2055-66.
- KOVANEN, P. E. & LEONARD, W. J. 2004. Cytokines and immunodeficiency diseases: critical roles of the gamma(c)-dependent cytokines interleukins 2, 4, 7, 9, 15, and 21, and their signaling pathways. *Immunol Rev*, 202, 67-83.
- KREBS, C., KOESTNER, W., NISSEN, M., WELGE, V., PARUSEL, I., MALAVASI, F., LEITER, E. H., SANTELLA, R. M., HAAG, F. & KOCH-NOLTE, F. 2003. Flow cytometric and immunoblot assays for cell surface ADP-ribosylation using a monoclonal antibody specific for ethenoadenosine. *Anal Biochem*, 314, 108-15.
- KRIEG, C., LETOURNEAU, S., PANTALEO, G. & BOYMAN, O. Improved IL-2 immunotherapy by selective stimulation of IL-2 receptors on lymphocytes and endothelial cells. *Proc Natl Acad Sci U S A*, 107, 11906-11.
- KRIEG, C., LETOURNEAU, S., PANTALEO, G. & BOYMAN, O. 2010. Improved IL-2 immunotherapy by selective stimulation of IL-2 receptors on lymphocytes and endothelial cells. *Proc Natl Acad Sci U S A*, 107, 11906-11.
- LAHL, K., LODDENKEMPER, C., DROUIN, C., FREYER, J., ARNASON, J., EBERL, G., HAMANN, A., WAGNER, H., HUEHN, J. & SPARWASSER, T. 2007. Selective depletion of Foxp3⁺ regulatory T cells induces a scurfy-like disease. *J Exp Med*, 204, 57-63.
- LAING, S., UNGER, M., KOCH-NOLTE, F. & HAAG, F. ADP-ribosylation of arginine. *Amino Acids*.
- LAING, S., UNGER, M., KOCH-NOLTE, F. & HAAG, F. 2010. ADP-ribosylation of arginine. *Amino Acids*.
- LEONARD, W. J., DEPPER, J. M., UCHIYAMA, T., SMITH, K. A., WALDMANN, T. A. & GREENE, W. C. 1982. A monoclonal antibody that appears to recognize the receptor for human T-cell growth factor; partial characterization of the receptor. *Nature*, 300, 267-9.
- LETOURNEAU, S., VAN LEEUWEN, E. M., KRIEG, C., MARTIN, C., PANTALEO, G., SPRENT, J., SURH, C. D. & BOYMAN, O. IL-2/anti-IL-2 antibody complexes show strong biological activity by avoiding interaction with IL-2 receptor alpha subunit CD25. *Proc Natl Acad Sci U S A*, 107, 2171-6.
- LIN, J. X. & LEONARD, W. J. 1997. Signaling from the IL-2 receptor to the nucleus. *Cytokine Growth Factor Rev*, 8, 313-32.

- LIPAROTO, S. F., MYSZKA, D. G., WU, Z., GOLDSTEIN, B., LAUE, T. M. & CIARDELLI, T. L. 2002. Analysis of the role of the interleukin-2 receptor gamma chain in ligand binding. *Biochemistry*, 41, 2543-51.
- MALEK, T. R. 2008. The biology of interleukin-2. *Annu Rev Immunol*, 26, 453-79.
- MATKO, J., BODNAR, A., VEREB, G., BENE, L., VAMOSI, G., SZENTESI, G., SZOLLOSI, J., GASPAR, R., HOREJSI, V., WALDMANN, T. A. & DAMJANOVICH, S. 2002. GPI-microdomains (membrane rafts) and signaling of the multi-chain interleukin-2 receptor in human lymphoma/leukemia T cell lines. *Eur J Biochem*, 269, 1199-208.
- MATTHES, M., HOLLMANN, C., BERTULEIT, H., KÜHL, M., THIELE, H. G., HAAG, F. & KOCH-NOLTE, F. 1997. "Natural" RT6-1 and RT6-2 "knock-out" mice. *Adv. Exp. Med. Biol.*, 419, 271-4.
- MÖLLER, M., JUNG, C., ADRIOUCH, S., DUBBERKE, G., SEYFRIED, F., SEMAN, M., HAAG, F. & KOCH-NOLTE, F. 2007. Monitoring the expression of purinoceptors and nucleotide-metabolizing ecto-enzymes with antibodies directed against proteins in native conformation. *Purinergic Signalling*, 3, 359-366.
- MOSS, J., STANLEY, S. J., NIGHTINGALE, M. S., MURTAGH, J. J., MONACO, L., MISHIMA, K., CHEN, H. C., WILLIAMSON, K. C. & TSAI, S. C. 1992. Molecular and immunological characterization of ADP-ribosylarginine hydrolases. *J Biol Chem*, 267, 10481-8.
- NAVARRO-MILLAN, I., SINGH, J. A. & CURTIS, J. R. 2012. Systematic review of tocilizumab for rheumatoid arthritis: a new biologic agent targeting the interleukin-6 receptor. *Clin Ther*, 34, 788-802 e3.
- NELSON, B. H., LORD, J. D. & GREENBERG, P. D. 1994. Cytoplasmic domains of the interleukin-2 receptor beta and gamma chains mediate the signal for T-cell proliferation. *Nature*, 369, 333-6.
- NELSON, B. H. & WILLERFORD, D. M. 1998. Biology of the interleukin-2 receptor. *Adv Immunol*, 70, 1-81.
- NEMOTO, E., YU, Y. & DENNERT, G. 1996. Cell surface ADP-ribosyltransferase regulates lymphocyte function- associated molecule-1 (LFA-1) function in T cells. *J Immunol*, 157, 3341-9.
- NORTH, R. A. 2002. Molecular physiology of P2X receptors. *Physiol Rev*, 82, 1013-67.
- OCHS, H. D., GAMBINERI, E. & TORGERSON, T. R. 2007. IPEX, FOXP3 and regulatory T-cells: a model for autoimmunity. *Immunol Res*, 38, 112-21.
- OHLROGGE, W., HAAG, F., LOHLER, J., SEMAN, M., LITTMAN, D. R., KILLEEN, N. & KOCH-NOLTE, F. 2002. Generation and characterization of ecto-ADP-ribosyltransferase ART2.1/ART2.2-deficient mice. *Mol Cell Biol*, 22, 7535-7542.
- OPPENHEIM, J. J. 2001. Cytokines: past, present, and future. *Int J Hematol*, 74, 3-8.
- PANDIYAN, P., ZHENG, L., ISHIHARA, S., REED, J. & LENARDO, M. J. 2007. CD4+CD25+Foxp3+ regulatory T cells induce cytokine deprivation-mediated apoptosis of effector CD4+ T cells. *Nat Immunol*, 8, 1353-62.

- PAONE, G., STEVENS, L. A., LEVINE, R. L., BOURGEOIS, C., STEAGALL, W. K., GOCHUICO, B. R. & MOSS, J. 2006. ADP-ribosyltransferase-specific modification of human neutrophil peptide-1. *J Biol Chem*, 281, 17054-60.
- RICKERT, M., BOULANGER, M. J., GORIATCHEVA, N. & GARCIA, K. C. 2004. Compensatory energetic mechanisms mediating the assembly of signaling complexes between interleukin-2 and its alpha, beta, and gamma(c) receptors. *J Mol Biol*, 339, 1115-28.
- ROBB, R. J., RUSK, C. M. & NEEPER, M. P. 1988. Structure-function relationships for the interleukin 2 receptor: location of ligand and antibody binding sites on the Tac receptor chain by mutational analysis. *Proc Natl Acad Sci U S A*, 85, 5654-8.
- ROGERS, W. O., WEAVER, C. T., KRAUS, L. A., LI, J., LI, L. & BUCY, R. P. 1997. Visualization of antigen-specific T cell activation and cytokine expression in vivo. *J Immunol*, 158, 649-57.
- ROIFMAN, C. M. 2000. Human IL-2 receptor alpha chain deficiency. *Pediatr Res*, 48, 6-11.
- RUSSELL, S. M., JOHNSTON, J. A., NOGUCHI, M., KAWAMURA, M., BACON, C. M., FRIEDMANN, M., BERG, M., MCVICAR, D. W., WITTHUHN, B. A., SILVENNOINEN, O. & ET AL. 1994. Interaction of IL-2R beta and gamma c chains with Jak1 and Jak3: implications for XSCID and XCID. *Science*, 266, 1042-5.
- SAADOUN, D., ROSENZWAJG, M., JOLY, F., SIX, A., CARRAT, F., THIBAUT, V., SENE, D., CACOUB, P. & KLATZMANN, D. 2011. Regulatory T-cell responses to low-dose interleukin-2 in HCV-induced vasculitis. *N Engl J Med*, 365, 2067-77.
- SAKAGUCHI, S., SAKAGUCHI, N., ASANO, M., ITOH, M. & TODA, M. 1995. Immunologic self-tolerance maintained by activated T cells expressing IL-2 receptor alpha-chains (CD25). Breakdown of a single mechanism of self-tolerance causes various autoimmune diseases. *J Immunol*, 155, 1151-64.
- SAKAGUCHI, S., YAMAGUCHI, T., NOMURA, T. & ONO, M. 2008. Regulatory T cells and immune tolerance. *Cell*, 133, 775-87.
- SCHEUPLEIN, F., SCHWARZ, N., ADRIOUCH, S., KREBS, C., BANNAS, P., RISSIEK, B., SEMAN, M., HAAG, F. & KOCH-NOLTE, F. 2009. NAD⁺ and ATP released from injured cells induce P2X7-dependent shedding of CD62L and externalization of phosphatidylserine by murine T cells. *J Immunol*, 182, 2898-908.
- SEMAN, M., ADRIOUCH, S., SCHEUPLEIN, F., KREBS, C., FREESE, D., GLOWACKI, G., DETERRE, P., HAAG, F. & KOCH-NOLTE, F. 2003. NAD-induced T cell death: ADP-ribosylation of cell surface proteins by ART2 activates the cytolytic P2X7 purinoceptor. *Immunity*, 19, 571-82.
- SHARFE, N., DADI, H. K., SHAHAR, M. & ROIFMAN, C. M. 1997. Human immune disorder arising from mutation of the alpha chain of the interleukin-2 receptor. *Proc Natl Acad Sci U S A*, 94, 3168-71.
- SHEVACH, E. M. 2009. Mechanisms of foxp3⁺ T regulatory cell-mediated suppression. *Immunity*, 30, 636-45.

- SOLLE, M., LABASI, J., PERREGAUX, D. G., STAM, E., PETRUSHOVA, N., KOLLER, B. H., GRIFFITHS, R. J. & GABEL, C. A. 2001. Altered cytokine production in mice lacking P2X(7) receptors. *J Biol Chem*, 276, 125-32.
- STAUBER, D. J., DEBLER, E. W., HORTON, P. A., SMITH, K. A. & WILSON, I. A. 2006. Crystal structure of the IL-2 signaling complex: paradigm for a heterotrimeric cytokine receptor. *Proc Natl Acad Sci U S A*, 103, 2788-93.
- SUGAMURA, K., ASAO, H., KONDO, M., TANAKA, N., ISHII, N., NAKAMURA, M. & TAKESHITA, T. 1995. The common gamma-chain for multiple cytokine receptors. *Adv Immunol*, 59, 225-77.
- SUN, J., MARESSO, A. W., KIM, J. J. & BARBIERI, J. T. 2004. How bacterial ADP-ribosylating toxins recognize substrates. *Nat Struct Mol Biol*, 11, 868-76.
- SUZUKI, H., KUNDIG, T. M., FURLONGER, C., WAKEHAM, A., TIMMS, E., MATSUYAMA, T., SCHMITS, R., SIMARD, J. J., OHASHI, P. S., GRIESSER, H. & ET AL. 1995. Deregulated T cell activation and autoimmunity in mice lacking interleukin-2 receptor beta. *Science*, 268, 1472-6.
- TAKESHITA, T., OHTANI, K., ASAO, H., KUMAKI, S., NAKAMURA, M. & SUGAMURA, K. 1992. An associated molecule, p64, with IL-2 receptor beta chain. Its possible involvement in the formation of the functional intermediate-affinity IL-2 receptor complex. *J Immunol*, 148, 2154-8.
- THEZE, J. 1994. Cytokine receptors: a combinative family of molecules. *Eur Cytokine Netw*, 5, 353-68.
- TORGERSON, T. R. & OCHS, H. D. 2007. Regulatory T cells in primary immunodeficiency diseases. *Curr Opin Allergy Clin Immunol*, 7, 515-21.
- TSUDO, M., KOZAK, R. W., GOLDMAN, C. K. & WALDMANN, T. A. 1987. Contribution of a p75 interleukin 2 binding peptide to a high-affinity interleukin 2 receptor complex. *Proc Natl Acad Sci U S A*, 84, 4215-8.
- TSUGE, H., NAGAHAMA, M., ODA, M., IWAMOTO, S., UTSUNOMIYA, H., MARQUEZ, V. E., KATUNUMA, N., NISHIZAWA, M. & SAKURAI, J. 2008. Structural basis of actin recognition and arginine ADP-ribosylation by *Clostridium perfringens* iota-toxin. *Proc Natl Acad Sci U S A*, 105, 7399-404.
- VLAD, G., HO, E. K., VASILESCU, E. R., FAN, J., LIU, Z., CAI, J. W., JIN, Z., BURKE, E., DENG, M., CADEIRAS, M., CORTESINI, R., ITESCU, S., MARBOE, C., MANCINI, D. & SUCIU-FOCA, N. 2007. Anti-CD25 treatment and FOXP3-positive regulatory T cells in heart transplantation. *Transpl Immunol*, 18, 13-21.
- WALDMANN, T. A. 2007. Daclizumab (anti-Tac, Zenapax) in the treatment of leukemia/lymphoma. *Oncogene*, 26, 3699-703.
- WEBSTER, K. E., WALTERS, S., KOHLER, R. E., MRKVAN, T., BOYMAN, O., SURH, C. D., GREY, S. T. & SPRENT, J. 2009. In vivo expansion of T reg cells with IL-2-mAb complexes: induction of resistance to EAE and long-term acceptance of islet allografts without immunosuppression. *J Exp Med*, 206, 751-60.
- WILDIN, R. S., RAMSDELL, F., PEAKE, J., FARAVELLI, F., CASANOVA, J. L., BUIST, N., LEVY-LAHAD, E., MAZZELLA, M., GOULET, O., PERRONI, L., BRICARELLI, F. D., BYRNE, G., MCEUEN, M., PROLL, S., APPLEBY,

- M. & BRUNKOW, M. E. 2001. X-linked neonatal diabetes mellitus, enteropathy and endocrinopathy syndrome is the human equivalent of mouse scurfy. *Nat Genet*, 27, 18-20.
- YASUKAWA, H., SASAKI, A. & YOSHIMURA, A. 2000. Negative regulation of cytokine signaling pathways. *Annu Rev Immunol*, 18, 143-64.
- ZHENG, L., TRAGESER, C. L., WILLERFORD, D. M. & LENARDO, M. J. 1998. T cell growth cytokines cause the superinduction of molecules mediating antigen-induced T lymphocyte death. *J Immunol*, 160, 763-9.
- ZOLKIEWSKA, A. 2005. Ecto-ADP-ribose transferases: cell-surface response to local tissue injury. *Physiology (Bethesda)*, 20, 374-81.

10 Acknowledgements

First and foremost, my utmost gratitude goes to Professor Dr. Friedrich Nolte, Institute of Immunology, University Medical Center Hamburg. His constant availability, encouragement, sharing of ideas, sense of perfection, patience, sincerity and care for his colleagues have made my time in the world of science an extremely valuable part of my medical career. Only through him was it possible to attend interesting conferences and even present results, be part of the graduate colleague “inflammation and regeneration” and get a stipend from the “Studienstiftung des Deutschen Volkes”. Prof. Koch-Nolte has the gift of taking his students seriously, no matter what experience they bring, but at the same time challenge them constantly which I admire and would like to pass on later in my career.

Prof. Giesa Tiegs, head of department of the institute for experimental immunology and hepatology, made it possible for me to attend the graduate school “inflammation and regeneration” together with 11 other medical student, which served as an additional inspiration and guide throughout my work on the thesis.

Thomas Jacobs, for being part of the graduate school supervision team.

I would like to thank all members of the IFI-lab, who shared valuable insights and always made me feel welcome in the laboratory.

Dr. Björn Rissiek, for his readiness to share his insights on animal experiments and FACS analyses and his assistance in mouse experiments, cell sorting methods, the STAT5 phosphorylation assay and the Interleukin-2 binding assay (Fig. 4.2) and for editing my dissertation.

Dr. Nicole Schwarz for her expertise regarding cell cultures, microscopy, antibody staining and FACS analyses

Dagmara Nelson for her assistance with radioactive labeling experiments using [³²P]-NAD⁺ (Fig. 4.3).

Alexander Hann for providing constructs for wildtype human CD25.

Fabienne Seyfried for her constant availability regarding practical laboratory work, for providing her P2X7 constructs and the pCMV-Sport6 vector, and helping with molecular biology techniques, especially minipreparation of plasmid DNA.

Marion Nissen for her expertise in cell cultures, CD25 constructs, immunoprecipitation and radioactive ADP-ribosylation assays.

Gudrun Dubberke for her assistance with western blots, cell culture and cell transfection.

Valea Schumacher for her help with PCR.

Janusz Wesolowski for his support with the applied molecular biology techniques including an introduction to all related software.

It would not have been possible to write this doctoral thesis without the support of the kind people around me who contributed in one way or another to the preparation and completion of this thesis. My family, especially my parents and my husband Tim Teege, have always been supportive throughout my medical studies whenever they could, especially by caring for our daughter Julie, but also my friends always had kind concern and consideration regarding my scientific work.

This thesis was funded in parts by grant No310/7-1 from the Deutsche Forschungsgemeinschaft and by a stipend from the graduate school „inflammation & regeneration“.

11 Curriculum vitae

Aus datenschutzrechtlichen Gründen gelöscht

-

-

-

-

-

-

-

12 Eidesstattliche Versicherung

[als letztes Blatt in die Dissertation einzubinden]

Ich versichere ausdrücklich, dass ich die Arbeit selbständig und ohne fremde Hilfe verfasst, andere als die von mir angegebenen Quellen und Hilfsmittel nicht benutzt und die aus den benutzten Werken wörtlich oder inhaltlich entnommenen Stellen einzeln nach Ausgabe (Auflage und Jahr des Erscheinens), Band und Seite des benutzten Werkes kenntlich gemacht habe.

Ferner versichere ich, dass ich die Dissertation bisher nicht einem Fachvertreter an einer anderen Hochschule zur Überprüfung vorgelegt oder mich anderweitig um Zulassung zur Promotion beworben habe.

Unterschrift: